RESEARCH ARTICLE

SATAY-based chemogenomic screening uncovers antifungal resistance mechanisms and key determinants of ATI-2307 and chitosan sensitivity

Matthew T Karadzas[1], Agnès H Michel[1], Andreas Mosbach[2], George Giannakopoulos[3], Ruairi McGettigan[1], Gabriel Scalliet[2], Benoit Kornmann[1]*

[1]Department of Biochemistry, University of Oxford, Oxford, United Kingdom; [2]Syngenta Crop Protection, Stein, Switzerland; [3]Syngenta Jealott's Hill Research Station, Bracknell, United Kingdom

eLife Assessment

This **important** manuscript proposes a new strategy for the identification of new mechanisms of drug resistance based on SAturated Transposon Analysis in Yeast (SATAY), a powerful transposon sequencing method in *Saccharomyces cerevisiae*. This method allows us to uncover loss- and gain-of-function mutations conferring resistance to 20 different antifungal compounds. The method is **convincing**, allowing the authors to identify a novel interaction of chitosan with the cell wall mannosylphosphate, and show that the transporter Hol1 concentrates the novel antifungal ATI-2307 within yeast.

***For correspondence:** benoit.kornmann@bioch.ox.ac.uk

Competing interest: The authors declare that no competing interests exist.

Funding: See page 21

Preprint posted
01 October 2024
Sent for Review
09 December 2024
Reviewed preprint v1
19 February 2025
Version of Record
23 November 2026

Reviewing Editor: Gustavo Henrique Goldman, Universidade de São Paulo, Brazil

© Copyright Karadzas *et al*. This article is distributed under the terms of the Creative Commons Attribution License, which permits unrestricted use and redistribution provided that the original author and source are credited.

Abstract Multidrug-resistant fungal pathogens are a serious threat to public health and global food security. Mitigation requires the discovery of antifungal compounds with novel modes of action along with a comprehensive understanding of the molecular mechanisms governing antifungal resistance. Here, we apply saturated transposon analysis in yeast (SATAY), a powerful transposon sequencing method in *Saccharomyces cerevisiae*, to uncover loss- and gain-of-function mutations conferring resistance to 20 different antifungal compounds. These screens identify a diverse array of novel resistance mechanisms and multiple modes of action. SATAY is performed in drug-sensitive strains to generate chemogenomic profiles for compounds that lack activity against conventional laboratory strains. This study therefore provides a significant resource for exploring cellular responses to chemical stresses. We discover that the natural antifungal chitosan electrostatically interacts with cell wall mannosylphosphate and that the transporter Hol1 concentrates the novel antifungal ATI-2307 within yeast. This latter finding presents an avenue for drug design initiatives but also unveils a straightforward evolutionary path to ATI-2307 resistance with minimal fitness cost.

Introduction

Fungal pathogens are a serious public health concern. Invasive fungal infections (IFIs) cause approximately 2.5 million deaths worldwide every year (***Denning, 2024***), and cases of IFIs are continuing to rise sharply, concomitant with the expanding population of immunocompromised individuals (***Bongomin et al., 2017***). Meanwhile, fungal plant pathogens pose the most serious biotic challenge to global food security (***Steinberg and Gurr, 2020***), accounting for approximately 20% of crop yield losses

pre-harvest and a further 10–20% post-harvest (**Fisher et al., 2018**). Fungal pathogens are currently controlled using a very limited number of antifungal compounds: only four classes of clinical antifungals are available (**Puumala et al., 2024**), whilst the agrochemical fungicide market comprises six main classes (**Fones et al., 2020**). Resistance to all these classes has emerged in major fungal pathogens, undermining our ability to control fungal infections in both clinical and agricultural settings (**Fisher et al., 2018**; **Perlin et al., 2017**). Meanwhile, our understanding of the molecular mechanisms responsible for antifungal resistance remains incomplete, yet this knowledge is critical for the development of effective resistance management strategies (**Robbins et al., 2017**). Furthermore, the scarcity of antifungal compounds demands concerted action towards the discovery of antifungals with novel modes of action (**Perfect, 2017**; **Puumala et al., 2024**).

Chemogenomic screening approaches in the model yeast *Saccharomyces cerevisiae* have accelerated the discovery of antifungal resistance mechanisms and modes of action (**Giaever et al., 1999**; **Giaever et al., 2004**; **Hoepfner et al., 2014**; **Lee et al., 2014**). These approaches involve the systematic identification of every gene that promotes antifungal sensitivity or resistance and are enabled by the fact that, unlike fungal pathogens, *S. cerevisiae* is easy to genetically manipulate, has an extensively annotated genome, a complete sexual cycle and grows rapidly on cheap medium under standard laboratory conditions (**Demuyser and Van Dijck, 2019**; **Duina et al., 2014**). Genome-wide yeast deletion collections (**Giaever et al., 2002**; **Winzeler et al., 1999**) have been successfully utilised for chemogenomic screening approaches such as haploinsufficiency profiling and homozygous profiling (**Giaever et al., 1999**; **Giaever et al., 2004**; **Hillenmeyer et al., 2008**; **Hoepfner et al., 2014**; **Parsons et al., 2004**). However, yeast deletion collections are only available in a small number of conventional laboratory strains, and since genetic background affects the penetrance and/or expression of genetic traits, this can complicate the connection from genotype to phenotype. These analyses are complicated further by the fact that many deletion collection strains have accumulated secondary mutations (**Teng et al., 2013**).

Recently, an innovative genome-wide screening approach, generically termed transposon sequencing (Tn-seq), has been developed in a variety of microorganisms, including *S. cerevisiae* (**Gale et al., 2020**; **Gao et al., 2018**; **Guo et al., 2013**; **Li et al., 2011**; **Mielich et al., 2018**; **Patterson et al., 2018**; **Sanchez et al., 2019**; **Segal et al., 2018**; **van Opijnen et al., 2009**; **Zhu et al., 2018**; **Edskes et al., 2018**; **Michel et al., 2017**). Tn-seq utilises random transposon mutagenesis to generate dense transposon libraries, in which every gene is disrupted by multiple independent transposon insertions. The insertion sites are identified en masse using next-generation sequencing, with the number of sequencing reads for each insertion reflecting the abundance of the corresponding mutants in the library population. When a library is grown under a test condition, the change in the number of reads for each insertion reveals the effect of the insertion on fitness (**van Opijnen et al., 2009**). In this way, transposon libraries treated with antimicrobial compounds can identify genes affecting drug susceptibility (**Coe et al., 2019**; **Gallagher et al., 2011**; **Li et al., 2023**; **Murray et al., 2015**). Indeed, recent studies have utilised Tn-seq in the fungal pathogen *Candida glabrata* to identify genes affecting susceptibility to fluconazole (**Gale et al., 2020**; **Gale et al., 2023**), micafungin (**Nickels et al., 2024**), and the calcineurin inhibitor FK506 (**Pavesic et al., 2024**). Tn-seq has also been used to explore the genetic basis of fluconazole susceptibility in *Candida albicans* (**Gao et al., 2018**). Tn-seq overcomes some of the main drawbacks of yeast deletion collections: transposon libraries are easily generated de novo, facilitating genome-wide screening in different genetic backgrounds (**Levitan et al., 2020**; **Michel et al., 2017**), and secondary mutations arising during Tn-seq do not confound data interpretation, since each gene is interrupted by multiple independent insertions (**Michel et al., 2017**).

Saturated transposon analysis in yeast (SATAY) is a powerful Tn-seq method in *S. cerevisiae* (**Chen et al., 2022**; **Michel et al., 2017**; **Michel and Kornmann, 2022**; **John Peter et al., 2022**) with significant potential for chemogenomic screening. Indeed, SATAY can simultaneously assess the fitness effects of loss- and gain-of-function mutations in different strains and test conditions in a labour- and time-efficient manner (**Michel et al., 2017**; **Serbyn et al., 2020**). Moreover, SATAY can be easily multiplexed (**John Peter et al., 2022**; **Michel and Kornmann, 2022**).

To address gaps in our understanding of antifungal resistance and modes of action, which is critical for future fungal disease control, we apply SATAY for chemogenomic screening of 20 antifungal compounds. This selection includes major classes of clinical and agrochemical antifungals, as well as experimental compounds, targeting a range of cellular processes, such as cell wall biosynthesis,

ergosterol biosynthesis, protein synthesis, glycosylation, and oxidative phosphorylation. The selection also includes compounds with unclear modes of action. Furthermore, by performing SATAY in drug-sensitive strains, we reveal the modes of action for compounds that lack activity against conventional laboratory strains, such as fludioxonil, iprodione, and chitosan. In addition, our screen with ATI-2307 unveils the genetic determinants underpinning the potency of this novel antifungal.

Results

SATAY can identify loss- and gain-of-function mutations conferring antifungal sensitivity or resistance

To evaluate the effectiveness of SATAY for chemogenomic screening, we performed a series of proof-of-principle screens with well-characterised antifungal compounds. Transposon libraries (***Supplementary file 1***) were grown for two successive rounds from OD_{600} 0.1–0.2 to saturation in the presence of sub-lethal concentrations of antifungal compounds inhibiting growth by about 30% (~IC_{30}) (***Supplementary file 2***). This concentration optimised the likelihood of identifying transposon insertions conferring antifungal resistance or sensitivity in the same screen (***Hoepfner et al., 2014***).

Transposon insertions interrupting the coding DNA sequence (CDS) of genes revealed loss-of-function mutations conferring antifungal resistance. For example, amphotericin B resistance was caused by transposons disrupting ergosterol homeostasis (***Figure 1A***, orange), the target of rapamycin complex 1 (TORC1) (***Figure 1A***, pink), and the TORC1-activating EGO complex (***Figure 1A***, blue), consistent with previous reports (***Bojsen et al., 2016***; ***Daum et al., 1999***; ***Martel et al., 2010***). Caspofungin resistance was conferred by transposons in sphingolipid biosynthesis genes (***Figure 1B***, orange) (***Supplementary file 3***), aligning with its known mode of action (***García et al., 2015***; ***Healey et al., 2012***; ***Satish and Perlin, 2019***). Caspofungin also positively selected transposons in *ERG3*, *LEM3*, *CRZ1*, and *GSC2* (***Figure 1B***, blue and pink), in agreement with previous findings (***García et al., 2015***; ***Lesage et al., 2004***; ***Markovich et al., 2004***). Myriocin, a potent inhibitor of serine palmitoyltransferase (***Miyake et al., 1995***), positively selected transposons in genes associated with cellular trafficking (***Figure 1C***: GARP complex, pink; retromer, teal; vesicular transport, orange), phospholipid translocation (***Figure 1C***, blue), and chromatin remodelling (***Figure 1C***, brown). Consistently, these genes have previously been associated with myriocin susceptibility (***Fröhlich et al., 2015***).

Antifungal resistance can also be conferred by gain-of-function mutations leading to target overexpression (***Robbins et al., 2017***). Given that the SATAY transposon bears cryptic promoter sequences (***Yu et al., 2004***), insertions in promoters can lead to downstream gene overexpression (***Serbyn et al., 2020***). We therefore wondered whether antifungal compounds might positively select transposons in the promoters of target genes. Since the annotation of promoters in *S. cerevisiae* is incomplete, we performed three separate analyses on insertions mapping within (1) 200 bp upstream of the ATG start codon, (2) 500 bp upstream of the ATG start codon, and (3) 200 bp upstream of the transcription start site, where known (***Xu et al., 2009***). For transposon libraries separately treated with cerulenin, fenpropimorph, prochloraz, or tunicamycin, the promoter regions containing the most enriched transposons were precisely those upstream of the genes encoding the corresponding targets: *FAS1* for cerulenin (***Johansson et al., 2008***), *ERG2* and *ERG24* for fenpropimorph (***Marcireau et al., 1990***), *ERG11* for prochloraz (***Becher and Wirsel, 2012***), and *ALG7* for tunicamycin (***Tkacz and Lampen, 1975***; ***Figure 1D***, red arrowheads) (***Figure 1—figure supplements 3–5***). This demonstrates that SATAY can be used to identify the direct targets of antifungal compounds.

In addition, our analysis of promoter regions revealed that SATAY can identify the drug efflux pumps responsible for detoxifying antifungal compounds (***Figure 1—figure supplements 3–5***). The overexpression of ATP-binding cassette (ABC) (***Prasad and Goffeau, 2012***) and major facilitator superfamily (MFS) transporters (***Sá-Correia et al., 2009***) is the basis for pleiotropic drug resistance (PDR) in *S. cerevisiae* (***Gulshan and Moye-Rowley, 2007***). We observed that transposons in the promoter of *PDR5*, encoding an ABC transporter (***Meyers et al., 1992***), were selected by cerulenin, fluconazole, prochloraz, and soraphen A (***Figure 1E***, pink arrowheads), all known Pdr5 substrates (***Arya et al., 2019***; ***Kolaczkowski et al., 1998***; ***Rogers et al., 2001***). Fluconazole and soraphen A also positively selected transposons in the promoter of *PDR3*, a transcription factor that regulates *PDR5* expression (***Moye-Rowley, 2003***; ***Sá-Correia et al., 2009***). Similarly, *SNQ2* promoter insertions were selected by fluazinam and fludioxonil (***Figure 1E***, pink arrowheads), suggesting that this ABC transporter

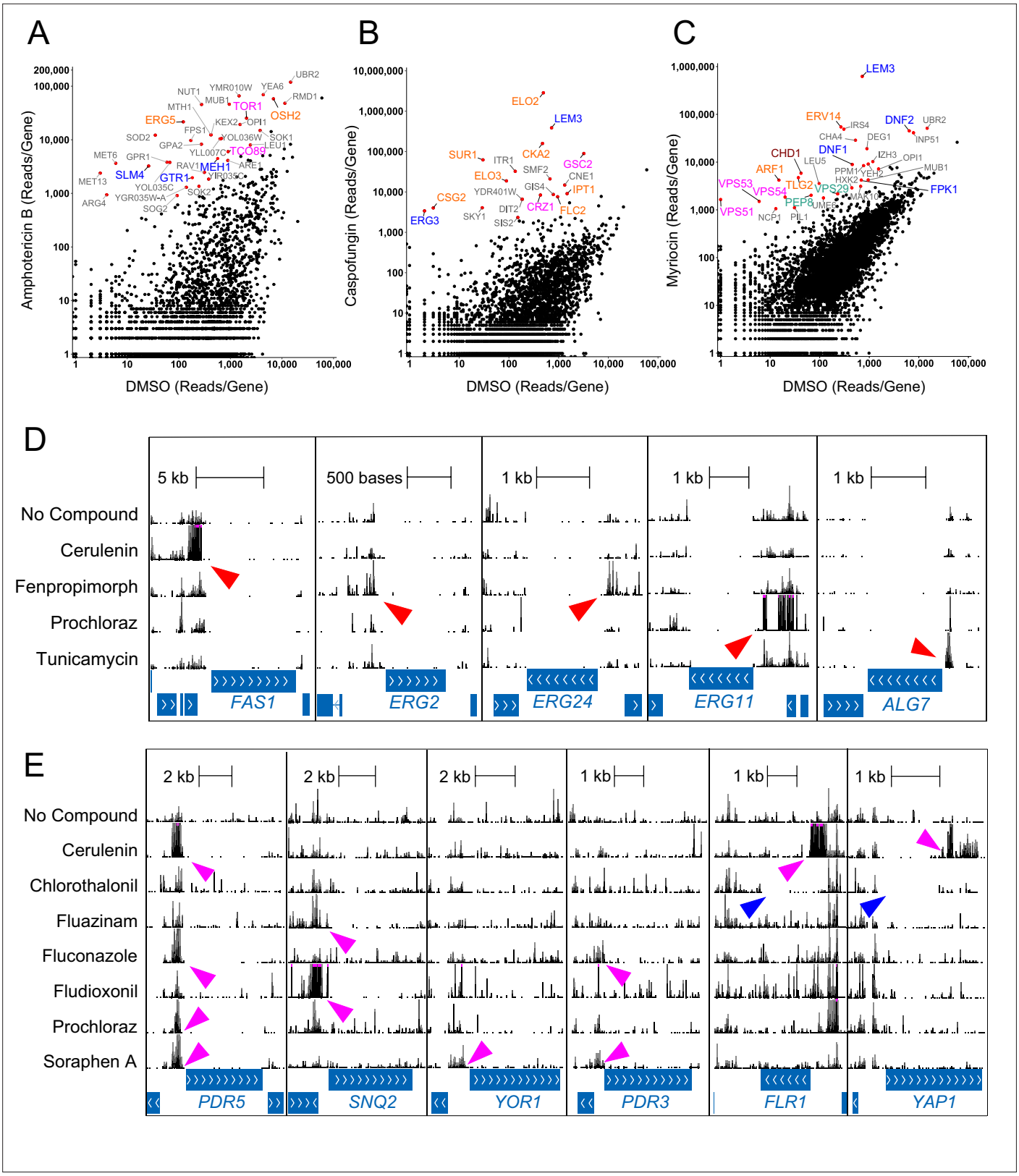


Figure 1. Saturated transposon analysis in yeast (SATAY) can identify loss- and gain-of-function mutations conferring antifungal sensitivity or resistance. (**A–C**) Scatter plots comparing the number of sequencing reads mapping to each of the 6603 yeast coding DNA sequences (CDSs) in transposon libraries treated with dimethyl sulfoxide (DMSO) versus (**A**) amphotericin B (0.375 µg/mL), (**B**) caspofungin (0.015 µg/mL), and (**C**) myriocin (0.2 µg/mL). Each dot represents a single gene. Gene names are colour-coded by biological process. (**A**) Orange – ergosterol homeostasis, pink – TORC1

Figure 1 continued on next page

Figure 1 continued

complex subunits, blue – EGO complex subunits. (**B**) Orange – sphingolipid biosynthesis, pink – β-1,3-glucan biosynthesis, blue – membrane lipid homeostasis. (**C**) Orange – vesicular-mediated transport, pink – GARP complex subunits, blue – phospholipid translocation, teal – retromer subunits, maroon – chromatin remodelling. (**D**) Transposon insertion maps for five antifungal drug targets. The height of the bars corresponds to the number of sequencing reads, shown on a linear scale that is capped at 500. Horizontal blue bars represent CDSs. Red arrowheads indicate positively selected insertions in the promoter regions of genes encoding drug targets. (**E**) Transposon insertion maps for four drug efflux pumps (*PDR5*, *SNQ2*, *YOR1*, *FLR1*) and two transcriptional regulators of the pleiotropic drug resistance (PDR) network (*PDR3*, *YAP1*). The height of the bars corresponds to the number of sequencing reads, shown on a linear scale that is capped at 500. Pink arrowheads indicate positively selected insertions in promoter regions or in the *YAP1* inhibitory domain. Blue arrowheads indicate regions of *FLR1* and *YAP1* where insertions were negatively selected.

The online version of this article includes the following figure supplement(s) for figure 1:

Figure supplement 1. Scatter plots comparing the number of transposons mapping in the coding DNA sequence (CDS) of every gene in transposon libraries treated with each compound.

Figure supplement 2. Scatter plots comparing the number of sequencing reads mapping in the coding DNA sequence (CDS) of every gene in transposon libraries treated with each compound.

Figure supplement 3. Scatter plots comparing the number of sequencing reads mapping to the promoters in transposon libraries treated with each compound.

Figure supplement 4. Scatter plots comparing the number of sequencing reads mapping to the promoters in transposon libraries treated with each compound.

Figure supplement 5. Scatter plots comparing the number of sequencing reads mapping to the promoters in transposon libraries treated with each compound.

(***Servos et al., 1993***) exports these compounds. Notably, the positive selection of transposons in the promoters of *PDR5* and *SNQ2* correlated with the negative selection of transposons in their CDSs.

Interestingly, SATAY reveals insights into the regulation of drug efflux pumps, which are only expressed under specific stress conditions. The loss of non-expressed pumps has no effect on fitness but, during drug treatments, their increased expression becomes beneficial, leading to positive selection of transposons in their promoters. This was evident for *FLR1*, which encodes an MFS transporter, after cerulenin treatment (***Figure 1E***, pink arrowheads; ***Oskouian and Saba, 1999***). Conversely, for efflux pumps that are sufficiently expressed, insertions in the promoter have little consequence, but insertions in the CDS are detrimental. This is the case for *FLR1* during chlorothalonil treatment, where insertions in the promoter are neutral, but insertions in the CDS are negatively selected (***Figure 1E***, blue arrowhead). We therefore conclude that *FLR1* expression is silent upon cerulenin treatment, but strong in chlorothalonil. *FLR1* is transcriptionally regulated by the redox-sensitive transcription factor Yap1 (***Alarco et al., 1997***; ***Jungwirth et al., 2000***). Yap1 contains a C-terminal inhibitory domain that is inactivated by oxidative stress (***Gulshan et al., 2005***; ***Kuge et al., 1997***). Accordingly, cerulenin favours insertions that truncate Yap1's C-terminus (***Figure 1E***, pink arrowhead), leading to its constitutive activation and subsequent *FLR1* overexpression (***Alarco et al., 1997***). Meanwhile, chlorothalonil likely activates Yap1 by inducing oxidative stress (***Tillman et al., 1973***). Supporting this, insertions in the N-terminal transcription activator region of *YAP1* CDS are negatively selected on chlorothalonil, while insertions in the inhibitory domain show no significant selection (***Figure 1E***, blue arrowhead). Therefore, the contrasting insertion profiles for *FLR1* and *YAP1* on cerulenin and chlorothalonil reveal the ability of Yap1 to sense chlorothalonil and its inability to sense cerulenin.

In summary, our proof-of-principle screens validate that SATAY is a robust approach for chemogenomic screening. We have demonstrated that SATAY can reveal loss- and gain-of-function mutations conferring antifungal resistance, the direct targets of antifungal compounds and the efflux pumps mediating drug export. Genes conferring resistance or sensitivity to all compounds screened in this study are shown in ***Figure 1—figure supplements 1–5***. Genomic maps of the transposon insertions can be browsed here:

- https://genome.ucsc.edu/s/Matthew%20Karadzas/Histograms_Karadzas%202024
- https://genome.ucsc.edu/s/Matthew%20Karadzas/Transposon_Maps_Karadzas_2024

SATAY can be performed in drug-sensitive strains of *S. cerevisiae*

Although *S. cerevisiae* is a powerful model for chemogenomic screening (***Robbins and Cowen, 2022***), it lacks sensitivity to several antifungal compounds. One reason for this is the PDR network

(**Kolaczkowski et al., 1998**), which can mask cellular responses relevant to a compound's mode of action and demands high levels of compound use. This is illustrated by our wild-type (ByK352) transposon library treated with 10 µg/mL prochloraz, an imidazole fungicide that is a substrate of the PDR network (**Kolaczkowski et al., 1998**). Indeed, most of the top-hits in this screen were associated with the Gene Ontology (GO) terms 'mitochondrial gene expression' and 'mitochondrial translation' (**Figure 2A**; **Supplementary file 3**) because mutations disrupting these functions activate the PDR network (**Hallstrom and Moye-Rowley, 2000**; **Zhang and Moye-Rowley, 2001**), increasing prochloraz detoxification.

We therefore assessed whether SATAY can be performed in a PDR-attenuated strain called 12geneΔ0HSR, in which eight ABC transporters and four transcriptional regulators of the PDR network have been deleted (**Chinen et al., 2011**). Consistently, 12geneΔ0HSR was 25-fold more sensitive towards prochloraz than the wild-type strain (ByK352) also derived from BY4741 (**Supplementary file 2**). Compared to the ByK352 transposon library, prochloraz positively selected transposons in an entirely different set of genes in the 12geneΔ0HSR transposon library (**Figure 2B**). Indeed, many of the top-hits were associated with the GO term 'vesicle-mediated transport' (**Supplementary file 3**). In fact, five of the most enriched genes (*MAK3*, *MAK10*, *ARL3*, *SYS1, ARL1*) all act in the same signalling pathway that culminates in the Golgi recruitment of Arl1, which promotes selective vesicle trafficking at the trans-Golgi network (**Behnia et al., 2004**; **Setty et al., 2003**; **Yu and Lee, 2017**). Similarly, a recent Tn-seq study in a PDR-attenuated strain of *C. glabrata* also observed that transposon insertions in genes with roles at the Golgi, including *MAK3* and *MAK10*, conferred fluconazole resistance (**Gale et al., 2023**). Thus, SATAY can be performed in PDR-attenuated strains to unveil PDR-independent resistance mechanisms at lower drug concentrations.

Another reason why *S. cerevisiae* lacks sensitivity to several compounds is that it does not express the corresponding target. Sensitivity can often be engineered by heterologously expressing the target in *S. cerevisiae*, and since SATAY can be performed in genetically engineered strains, it is a promising approach for the chemogenomic analysis of these compounds (**John Peter et al., 2022**; **Michel et al., 2017**). The fungicides fludioxonil and iprodione lack activity against *S. cerevisiae* (**Kilani and Fillinger, 2016**; **Leroux et al., 1992**; **Motoyama et al., 2005**). In filamentous fungi, these compounds are sensed by group III hybrid histidine kinases (HHKs), leading to the constitutive activation of the high osmolarity glycerol (HOG) signalling pathway, which is lethal (**Fillinger et al., 2012**; **Furukawa et al., 2012**; **Motoyama et al., 2005**; **Kojima et al., 2004**; **Zhang et al., 2002**). There are conflicting ideas regarding how fludioxonil affects group III HHKs, and a recent model proposes that fludioxonil does not target group III HHKs directly, but via an upstream factor of unclear identity (**Lawry et al., 2017**). *S. cerevisiae* does not harbour group III HHKs, but encodes one essential group VI HHK called Sln1 (**Catlett et al., 2003**; **Maeda et al., 1994**; **Ota and Varshavsky, 1993**; **Posas et al., 1996**). *S. cerevisiae* strains heterologously expressing a group III HHK are sensitive to fludioxonil and iprodione (**Buschart et al., 2012**; **Furukawa et al., 2012**; **Lawry et al., 2017**; **Meena et al., 2010**; **Motoyama et al., 2005**), indicating that if fludioxonil indeed acts upon an upstream factor, it must be present in *S. cerevisiae*, and SATAY might therefore be an appropriate way to identify it. We expressed a group III HHK called Drk1 from the fungal pathogen *Blastomyces dermatitidis* (**Nemecek et al., 2006**) in *S. cerevisiae*, which complemented the otherwise lethal deletion of *SLN1* (**Figure 2C**). We found that *sln1Δ BdDRK1* strains are equally susceptible to fludioxonil and iprodione as *SLN1 BdDRK1* strains (**Figure 2D**), consistent with reports that fludioxonil activates the HOG pathway in a dominant manner (**Lawry et al., 2017**; **Randhawa et al., 2019**). We generated a transposon library in an *sln1Δ BdDRK1* strain, in which the absence of Sln1 ensured that fludioxonil and iprodione resistance could not result from loss of *BdDRK1*.

Fludioxonil and iprodione strongly selected insertions in the five non-essential components of the HOG pathway (*SSK1*, *SSK2*, *SSK22*, *PBS2*, and *HOG1*) in the *sln1Δ BdDRK1* transposon library (**Figure 2E and F**, blue) (**Hohmann, 2002**). This aligns with studies showing that mutations in HOG pathway components confer fludioxonil and iprodione resistance (**Buschart et al., 2012**; **Furukawa et al., 2012**; **Kojima et al., 2004**; **Motoyama et al., 2005**; **Zhang et al., 2002**). We also observed that fludioxonil and iprodione selected transposons in subunits of the RNA polymerase II holoenzyme (*SSN8*) and mediator complex (*SSN2*, *SRB8*), subunits of the INO80 chromatin remodelling complex (*IES5*, *NHP10*) (**Figure 2E and F**, orange and pink) and in the transcriptional regulator gene *TUP1* (**Figure 2E and F**, orange), which recruits the SAGA histone acetylase and SWI/SNF nucleosome-remodelling

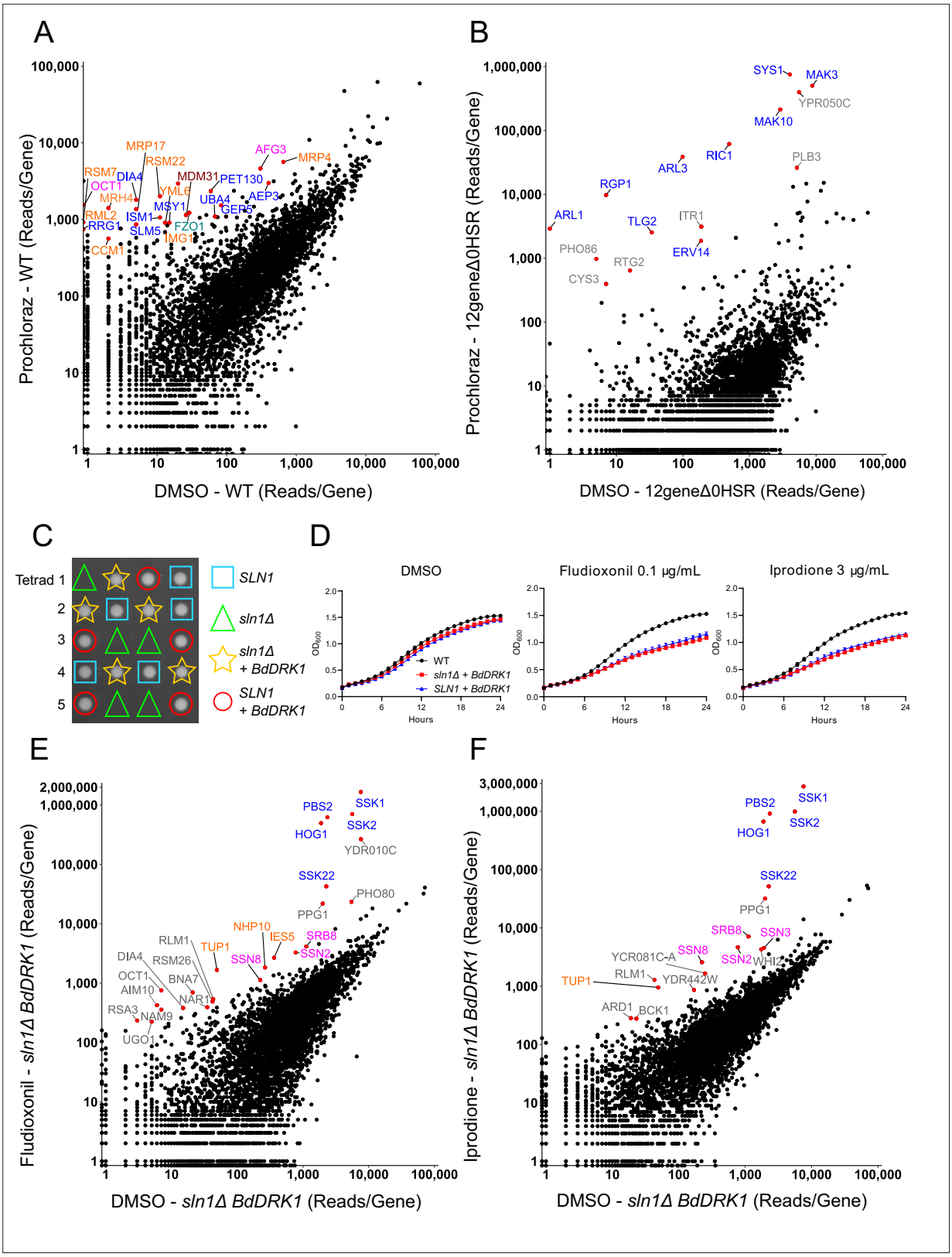


Figure 2. Saturated transposon analysis in yeast (SATAY) can be performed in drug-sensitive strains of *S. cerevisiae*. (**A**) Scatter plot comparing the number of sequencing reads mapping to each of the 6603 yeast coding DNA sequences (CDSs) in a pleiotropic drug resistance (PDR)-proficient transposon library treated with dimethyl sulfoxide (DMSO) versus prochloraz (10 µg/mL). Each dot represents a single gene. Gene names are colour-coded by biological process: orange – mitochondrial gene expression, blue – mitochondrial translation, pink – mitochondrial protein processing, teal –

Figure 2 continued on next page

Figure 2 continued

mitochondrial genome maintenance, maroon – mitochondrial phospholipid homeostasis. (**B**) As in (**A**), for a PDR-attenuated (12geneΔ0HSR) transposon library treated with DMSO versus prochloraz (0.4 µg/mL). Genes involved with vesicle-mediated transport are coloured blue. (**C**) Tetrad dissection of *SLN1/sln1Δ BdDRK1*±heterozygote on YPD medium. The genotypes of the non-growing spores have been inferred from the genotypes of the growing ones, assuming a Mendelian meiotic segregation pattern. (**D**) Growth curves of wild-type, *sln1Δ BdDRK1* and *SLN1 BdDRK1* strains in SC 2% glucose medium containing either 1% DMSO (vol/vol), fludioxonil (0.1 µg/mL), or iprodione (3 µg/mL). OD_{600} measurements were recorded every 20 min using a Bioscreen C instrument. Each data point is the mean OD_{600} measurement for three independent biological replicates. Error bars show standard error of mean (SEM). (**E–F**) Scatter plots comparing the number of sequencing reads mapping to each of the 6603 yeast CDSs in a *sln1Δ BdDRK1* transposon library treated with (**E**) fludioxonil (0.1 µg/mL) or (**F**) iprodione (3 µg/mL). Gene names are colour-coded by biological process: blue – high osmolarity glycerol (HOG) signalling pathway, pink – RNA polymerase holoenzyme or mediator complex subunit, orange – chromatin remodelling. Note that *YDR010C* is a dubious open reading frame (ORF) located in the promoter of the drug-efflux pump *SNQ2* (***Figure 1E***).

The online version of this article includes the following source data for figure 2:

Source data 1. Source data for ***Figure 2D***.

complex to stress-regulated promoters following Hog1 activation (***Conaway and Conaway, 2009***; ***Myer and Young, 1998***; ***Proft and Struhl, 2002***). Transposons in these genes likely disrupted the transcriptional reprogramming activities of Hog1 (***Alepuz et al., 2003***; ***Klopf et al., 2009***; ***Mas et al., 2009***; ***Nadal-Ribelles et al., 2012***; ***Zapater et al., 2007***), thereby suppressing the toxic effects of constitutive Hog1 activation. We did not observe any positive or negative selection for transposons inserted into genes previously proposed to act upstream of HHKs upon fludioxonil treatment, such as genes affecting mitochondrial activity, glutathione homeostasis, or aldehyde metabolism (***Brandhorst et al., 2019***). This argues against the idea that fludioxonil targets a factor upstream of group III HHKs. Together, this example demonstrates that SATAY can be performed in strains heterologously expressing antifungal drug targets, providing a straightforward way to screen antifungals with targets absent in *S. cerevisiae*.

Chitosan electrostatically interacts with cell wall mannosylphosphate

Having established that SATAY can identify antifungal resistance mechanisms and targets, we applied SATAY to examine chitosan. Chitosan is a natural polysaccharide derived from the deacetylation of chitin (***Kong et al., 2010***) and is used to control numerous pre- and post-harvest fungal diseases (***Bautista-Baños et al., 2006***), but has an unclear mode of action. Chitosan's activity is pH-dependent: at physiological pH, the amino groups in chitosan are partially protonated (***Figure 3A***; ***Ke et al., 2021***) and probably interact electrostatically with the cell surfaces of bacteria and fungi, increasing membrane permeability and causing metabolite leakage (***Helander et al., 2001***; ***Liu et al., 2004***; ***Mellegård et al., 2011***; ***Palma-Guerrero et al., 2010***; ***Palmeira-de-Oliveira et al., 2011***; ***Raafat et al., 2008***; ***Tayel et al., 2010***; ***Tsai and Su, 1999***). However, the specific targets for chitosan on fungal cell surfaces have not been identified (***Li et al., 2022***; ***Ma et al., 2017***; ***Shih et al., 2019***).

Despite having a broad antimicrobial spectrum (***Goy et al., 2009***; ***Ke et al., 2021***), chitosan has minimal activity against *S. cerevisiae* strains derived from the widely used laboratory strain S288C, such as BY4741 (***Jaime et al., 2012***; ***Zakrzewska et al., 2005***; ***Zakrzewska et al., 2007***). As yeast deletion collections were constructed in S288C (***Giaever et al., 2002***; ***Winzeler et al., 1999***), chemogenomic studies using yeast deletion collections have evaluated chitosan's mode of action at high concentrations, limiting physiological and agricultural relevance (***Galván Márquez et al., 2013***; ***Jaime et al., 2012***; ***Zakrzewska et al., 2007***). However, as SATAY is not tied to a specific genetic background (***Michel et al., 2017***), we assessed the sensitivity of several *S. cerevisiae* strains to chitosan. Chitosan susceptibility was observed for AD12345678 (hereafter AD1-8) (***Figure 3B***). AD1-8 is derived from a non-conventional strain called US50-18C and lacks seven ABC transporters and the transcription factor *PDR3* (***Decottignies et al., 1998***; ***Supplementary file 4***). Notably, S288C-derived strains lacking the same ABC transporters as AD1-8 (***Chinen et al., 2011***; ***Hoepfner et al., 2014***; ***Suzuki et al., 2011***) were not sensitive to chitosan (***Figure 3B***), indicating that AD1-8's chitosan sensitivity was not attributable to the disruption of the PDR network, but to unknown characteristics of the US50-18C background.

We treated an AD1-8 transposon library with 2 µg/mL chitosan and the corresponding acetic acid control. Chitosan caused a striking enrichment of transposons in genes associated with the GO terms 'glycoprotein biosynthetic process' and 'Golgi vesicle transport' (***Supplementary file 3***). These

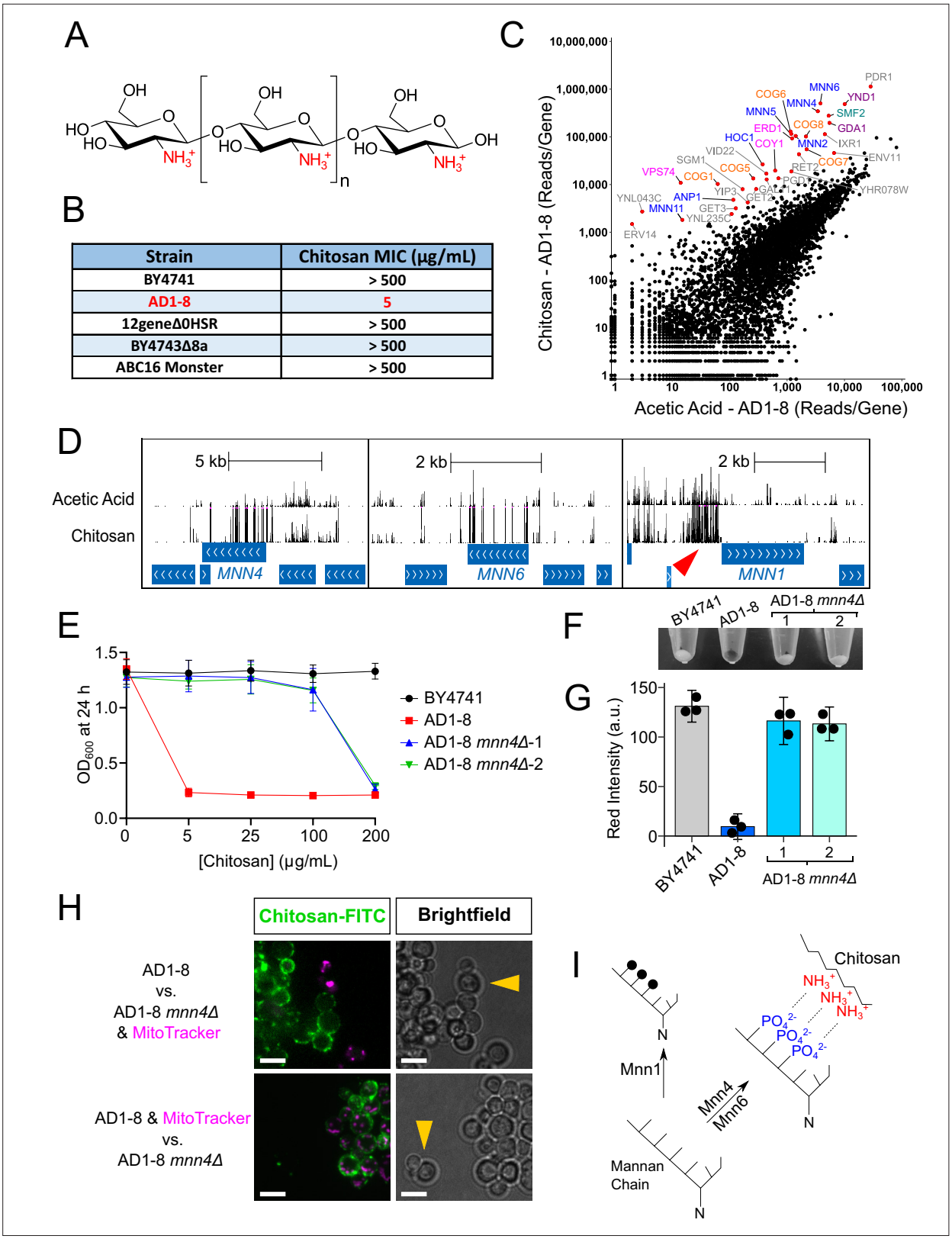


Figure 3. Chitosan electrostatically interacts with cell wall mannosylphosphate. (**A**) Chemical structure of chitosan. Protonated amino groups are shown in red. (**B**) Minimal inhibitory concentrations (MICs) of chitosan for five strains of *S. cerevisiae*. All strains are pleiotropic drug resistance (PDR)-attenuated except for BY4741. MICs were determined after 24 hr for SC 2% glucose cultures incubated at 30°C, 200 rpm. Note in this figure, BY4741 refers to ByK352 (***Supplementary file 4***). (**C**) Scatter plot comparing the number of sequencing reads mapping to each of the 6603 yeast coding DNA

Figure 3 continued on next page

Figure 3 continued

sequences (CDSs) for an AD1-8 transposon library treated with acetic acid (0.0004%) or chitosan (2 µg/mL). Gene names are colour-coded by biological process: blue – mannan chain elaboration on N-glycans of cell wall proteins; orange – conserved oligomeric Golgi (COG) complex subunits; pink – intra-Golgi retrograde transport; purple – nucleoside phosphatases required for GDP-mannose transport into the Golgi; teal – manganese transport. (**D**) Transposon insertion map for *MNN4, MNN6,* and *MNN1* in the AD1-8 transposon library following treatments with acetic acid (0.0004% [vol/vol]) and chitosan (2 µg/mL). The height of the bars corresponds to the number of sequencing reads, shown on a linear scale that is capped at 2000. Horizontal blue bars represent CDSs. Red arrowhead indicates positively selected insertions in the promoter region of *MNN1*. (**E**) Growth inhibition curves of a BY4741 strain, AD1-8, and two independent AD1-8 *mnn4Δ* strains treated with chitosan in SC 2% glucose medium. OD_{600} measurements were recorded using a Bioscreen C instrument set at 30°C, continuous shaking. Each data point is the mean OD_{600} measurement for three technical replicates. Error bars show the standard deviation. (**F**) Alcian blue staining of a BY4741 strain, AD1-8, and two independent AD1-8 *mnn4Δ* strains. Saturated cultures were treated with 10 µg/mL alcian blue solution in SC 2% glucose medium for 3 min. Image is displayed in the red channel, since alcian blue strongly absorbs red light. (**G**) Quantification of background-subtracted red channel intensity of alcian blue-stained pellets of BY4741 strain, AD1-8, and two independent AD1–8 *mnn4Δ* strains. Three technical replicates for each strain. Error bars show the standard deviation. (**H**) Representative images of AD1-8 and AD1-8 *mnn4Δ* strains following treatment with 25 µg/mL fluorescein-labelled chitosan (green) for 2 hr in SC 2% glucose medium. Cells were treated in stationary phase. MitoTracker (magenta) was applied at 0.1 µM. Yellow arrowheads indicate representative AD1-8 *mnn4Δ* cells. Images are Z-stacks. Scale bars represent 5 µm. (**I**) Model for the mechanism by which chitosan binds to the yeast cell wall. Model depicts electrostatic interactions (black dashes) between chitosan's positively charged amino groups (red) and negatively charged mannosylphosphate groups (blue) on an N-linked glycan chain. Mannosylphosphate groups are added onto α1,2-linked mannose side branches by the mannosylphosphate transferases Mnn4 and Mnn6. Meanwhile, Mnn1 adds terminal α1,3-linked mannose residues (black circles) to α1,2-linked mannose side chains. Terminal α1,3-linked mannose residues compete with mannosylphosphate groups for available α1,2-linked mannose acceptor sites. *MNN1* overexpression in AD1-8 likely conferred chitosan resistance by tipping this competition towards non-phosphorylated α1,3-linked mannose residues.

The online version of this article includes the following source data and figure supplement(s) for figure 3:

Source data 1. Source data for ***Figure 3E***.

Source data 2. Source data for the bar plot in ***Figure 3G***.

Figure supplement 1. Growth inhibition curves of a BY4741 strain (ByK352), AD1-8, and two independent *mnn4Δ* AD1-8 strains treated with acetic acid in SC 2% glucose medium.

Figure supplement 1—source data 1. Acetic acid sensitivity data used to compute ***Figure 3—figure supplement 1***.

Figure supplement 2. Representative images of AD1-8 and a BY4741 strain (ByK352) following treatment with 25 µg/mL chitosan fluorescein (green) for 2 hr in stationary phase in SC 2% glucose medium.

included genes encoding Golgi-localised mannosyltransferases or mannosylphosphate transferases (***Figure 3C***, blue), which are responsible for elongating and modifying N-linked glycans on cell wall proteins (***Munro, 2001***). Additionally, chitosan positively selected transposons in *GDA1* and *YND1* (***Figure 3C***, purple), which encode homologous Golgi-localised nucleoside phosphatases required for the transport of GDP-mannose into the Golgi lumen (***Berninsone et al., 1994***; ***Gao et al., 1999***). Chitosan also enriched transposons in the CDS of *SMF2* (***Figure 3C***, green), which encodes a manganese (Mn^{2+}) transporter necessary for the delivery of Mn^{2+} to the Golgi (***Luk and Culotta, 2001***). Consistently, Mn^{2+} is a critical co-factor for Ynd1 and Golgi-localised mannosyltransferases (***Gao et al., 1999***; ***Kuhn et al., 1991***; ***Nakajima and Ballou, 1975***). There was also a significant enrichment of transposons in *VPS74*, *ERD1*, *COY1* and five of the eight subunits of the conserved oligomeric Golgi (COG) complex (***Figure 3C***, pink and orange). These genes participate in intra-Golgi retrograde transport, which recycles glycosyltransferases from *trans*-Golgi to *cis/medial*-Golgi compartments, thereby maintaining their steady-state distribution. This is critical for ensuring the distinct steps of glycosylation occur in the correct sequential order (***Bruinsma et al., 2004***; ***Pokrovskaya et al., 2011***; ***Sardana et al., 2021***; ***Shestakova et al., 2006***). Thus, our SATAY screen strongly indicates that chitosan sensitivity in AD1-8 is engendered by the mannosylation of N-linked glycans on cell wall proteins, consistent with chitosan interacting with the fungal cell wall (***Li et al., 2022***; ***Tayel et al., 2010***).

Mannan chains on cell wall proteins are modified with phosphate groups, giving a net negative charge to the yeast cell wall (***Karson and Ballou, 1978***). We hypothesised that chitosan might electrostatically interact with mannosylphosphate. This hypothesis is supported by multiple findings in our SATAY screen. First, transposons disrupting genes required for mannosylphosphate transfer, *MNN4* (***Odani et al., 1996***) and *MNN6* (***Karson and Ballou, 1978***; ***Wang et al., 1997***), were strongly enriched by chitosan (***Figure 3C–E***). Second, several genes acting upstream of *MNN4* and *MNN6* contained strongly selected transposons, namely *ANP1*, *MNN11*, *HOC1*, *MNN2*, and *MNN5* (***Figure 3C***; ***Munro, 2001***; ***Orlean, 2012***). These upstream genes are necessary for the addition of α1,2-linked mannose side branches, which are the sole substrates of Mnn4 and Mnn6 (***Karson and Ballou, 1978***). Third,

chitosan positively selected transposons in the promoter region of *MNN1* (**Figure 3D**, red arrowhead, **Figure 1—figure supplement 3A**) and negatively selected transposons in the CDS of this gene. Mnn1 adds terminal α1,3-linked mannose residues to α1,2-linked mannose side chains (**Raschke et al., 1973**; **Yip et al., 1994**). As such, terminal α1,3-linked mannose residues compete with mannosylphosphate groups for available acceptor sites (**Karson and Ballou, 1978**). Thus, *MNN1* overexpression likely conferred chitosan resistance in AD1-8 by tipping this competition towards non-phosphorylated α1,3-linked mannose residues (**Figure 3I**).

Alcian blue is a cationic dye that can distinguish yeasts with different cell wall mannosylphosphate compositions (**Ballou, 1990**). AD1-8 cells were strongly stained by alcian blue, and this staining was dependent on *MNN4* (**Figure 3F and G**). In contrast, despite being wild-type for *MNN4*, the chitosan-resistant lab strain BY4741 did not bind alcian blue. This shows that levels of cell wall mannosylphosphate correlated with chitosan sensitivity, supporting the model that they interact electrostatically. Finally, our model implies that chitosan sensitivity and resistance are determined by different abilities to bind chitosan. To test this, we treated cells with fluorescein-labelled chitosan. To directly compare the fluorescence staining intensities on the same images, strains were mixed pairwise after staining and then imaged. The strains were distinguishable because only one strain received a pre-treatment with the unrelated vital stain, MitoTracker. Fluorescein-labelled chitosan strongly stained the cell walls of AD1-8 WT cells but failed to bind the cell walls of AD1-8 *mnn4Δ* cells (**Figure 3H**) or BY4741 cells (**Figure 3—figure supplement 2**). This further indicates that chitosan exerts its fungistatic effect by binding mannosylphosphate on the cell-surface (**Figure 3I**). Our study therefore identifies a mode of action for chitosan on fungal cell walls.

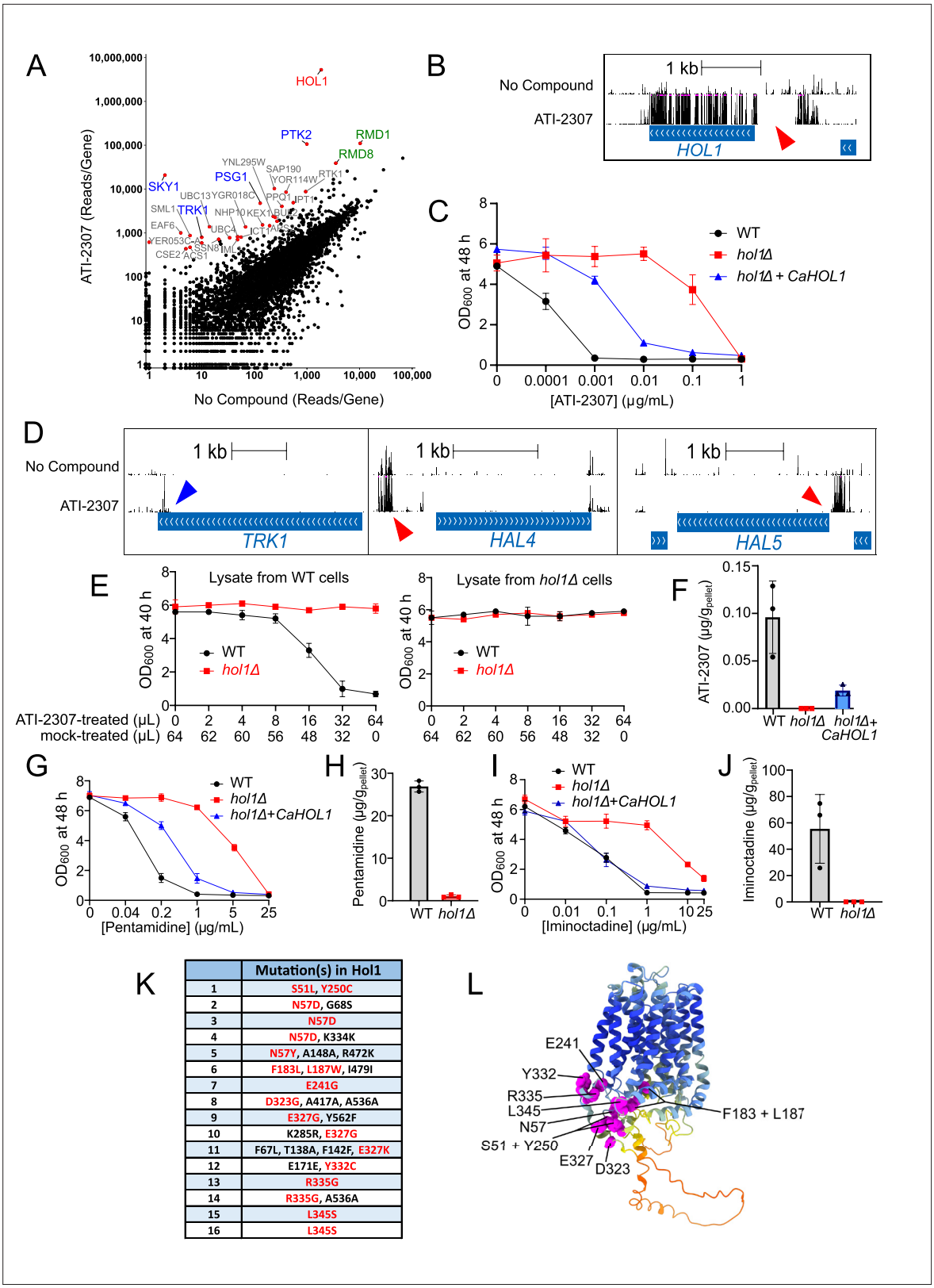
Hol1 imports ATI-2307, pentamidine, and iminoctadine into *S. cerevisiae*

ATI-2307 (formerly T-2307) is a novel antifungal with an unclear mode of action (**Wiederhold, 2021**). ATI-2307 exhibits broad-spectrum in vitro and in vivo activity against many clinically important fungal pathogens, including fluconazole-resistant strains of *C. albicans* and echinocandin-resistant *Candida* spp. (**Mitsuyama et al., 2008**; **Wiederhold et al., 2020**; **Nishikawa et al., 2017**; **Wiederhold et al., 2015**; **Wiederhold et al., 2016**). ATI-2307 therefore represents a promising compound for the future control of fungal infections.

ATI-2307 specifically inhibits *S. cerevisiae* in non-fermentative growth conditions (**Shibata et al., 2012**). Upon challenging a wild-type transposon library with ATI-2307 in non-fermentative medium, we identified multiple genes affecting susceptibility to this compound. Notably, genes causing ATI-2307 hypersensitivity when interrupted by transposons were significantly associated with the GO term 'regulation of gluconeogenesis' (**Supplementary file 3**). This included subunits of the GID (Glucose Induced degradation Deficient) complex, namely *GID7, GID8, VID28,* and *VID30* (**Figure 1—figure supplement 1A**, top-right panel). GID is an E3 ligase that polyubiquitylates fructose-1,6-bisphosphatase when non-fermenting cells encounter glucose (**Regelmann et al., 2003**). *UBC8* was also identified, which encodes a ubiquitin-conjugating enzyme that regulates the activity of the GID complex (**Regelmann et al., 2003**; **Schüle et al., 2000**). Moreover, transcription factors regulating the expression of gluconeogenic genes were essential on ATI-2307, namely *RDS2* (**Soontorngun et al., 2007**) and *ERT1* (**Gasmi et al., 2014**; **Figure 1—figure supplement 1A**, top-right panel). The connection between gluconeogenesis and ATI-2307 susceptibility remains unclear, but the enrichment of these functionally related hits underlines the specificity and comprehensiveness of the screen.

Among the genes causing ATI-2307 resistance when disrupted by transposons were the paralogs *RMD1* and *RMD8* (**Figure 4A**, green). Very little is known about the function of these genes, but they are homologous to a third protein, Mrx10, an inner mitochondrial membrane component of MIOREX complexes, large assemblies that spatially organise mitochondrial protein synthesis (**Kehrein et al., 2015**). Although Mrx10 was not identified by the SATAY screen, the homology to Rmd1 and Rmd8 is notable because mitochondrial protein synthesis is required for the biogenesis of respiratory complexes, which were previously implicated as targets for ATI-2307 (**Yamashita et al., 2019**).

The CDS of *HOL1* contained the most strongly selected transposon insertions (**Figure 4A and B**). Additionally, transposons mapping upstream of *HOL1*, in a region that negatively regulates *HOL1* expression in a post-transcriptional manner (**Vindu et al., 2021**; **Wright et al., 1996**), were negatively selected by ATI-2307 (**Figure 4B**, red arrowhead). These findings indicate that Hol1 engenders



	Mutation(s) in Hol1
1	S51L, Y250C
2	N57D, G68S
3	N57D
4	N57D, K334K
5	N57Y, A148A, R472K
6	F183L, L187W, I479I
7	E241G
8	D323G, A417A, A536A
9	E327G, Y562F
10	K285R, E327G
11	F67L, T138A, F142F, E327K
12	E171E, Y332C
13	R335G
14	R335G, A536A
15	L345S
16	L345S

Figure 4. Hol1 imports ATI-2307, pentamidine, and iminoctadine into *S. cerevisiae*. (**A**) Scatter plot comparing the number of sequencing reads mapping to each of the 6603 yeast coding DNA sequences (CDSs) in a transposon library after a control treatment versus ATI-2307 treatment (0.000175 µg/mL) in SC-TRP 2% ethanol medium. *HOL1* is coloured red. Genes involved in the regulation of the proton-motive force are coloured blue. *RMD1* and *RMD8* are coloured green. (**B**) Transposon insertion map for *HOL1* for the control and ATI-2307 treatments. The height of the bars

Figure 4 continued on next page

Figure 4 continued

corresponds to the number of sequencing reads, shown on a linear scale that is capped at 500. Red arrowhead indicates region upstream of *HOL1* where transposon insertions were negatively selected by ATI-2307. This region negatively regulates *HOL1* expression in a post-transcriptional manner (***Vindu et al., 2021***). (**C**) Growth inhibition curves for wild-type (WT), *hol1Δ* and *hol1Δ CaHOL1* strains treated with ATI-2307. WT and *hol1Δ* strains were transformed with pRS316 empty vector. OD_{600} measurements were recorded after 48 hr of growth in SC-URA 2% ethanol medium at 30°C, 200 rpm. Each data point is the mean OD_{600} measurement for three independent biological replicates. Error bars show the standard deviation. Error bars for some measurements were too small to be displayed. (**D**) Transposon insertion maps for *TRK1*, *HAL4*, and *HAL5* after the control and ATI-2307 treatments. The height of the bars corresponds to the number of sequencing reads, shown on a linear scale that is capped at 500. Blue arrowhead indicates positively selected insertions in the 3′-end of *TRK1*. Red arrowheads indicate positively selected insertions in the promoter regions of *HAL4* and *HAL5*. (**E**) Growth inhibition curves for WT and *hol1Δ* strains treated with lysate derived from ATI-2307-treated WT or *hol1Δ* cells. OD_{600} measurements were recorded after 40 hr of growth in SC 2% ethanol medium at 30°C, 200 rpm. Each data point is the mean of two independent biological replicates. Each culture was inoculated with a total of 64 µL lysate derived from WT or *hol1Δ* cells. The volume of lysate from ATI-2307-treated versus mock-treated cells is indicated on the x-axis. Error bars show the standard deviation. (**F**) Liquid chromatography-mass spectrometry (LC-MS) analysis of ATI-2307 uptake in WT, *hol1Δ* and *hol1Δ CaHOL1* cells. Cells were cultured in 200 mL SC 2% ethanol at 30°C, 200 rpm from a starting OD_{600} 0.5. Upon reaching OD_{600} 1, cells were treated for 2 hr with ATI-2307 (0.003 µg/mL). The *hol1Δ* strains expressing *CaHOL1* (pBK994) were grown in SC-URA 2% ethanol medium. Quantifications of ATI-2307 were performed using matrix-matched calibration curves. Each dot represents an independent biological replicate (n=3). Error bars show the standard deviation. (**G**) Growth inhibition curves for WT, *hol1Δ* and *hol1Δ CaHOL1* strains treated with pentamidine, as in (**C**). (**H**) LC-MS analysis of pentamidine uptake in WT or *hol1Δ* cells. Cells were treated with 1 µg/mL pentamidine. Other experiment details are identical to those described for ATI-2307 in (**F**). (**I**) Growth inhibition curves for WT, *hol1Δ* and *hol1Δ CaHOL1* strains treated with iminoctadine, as in (**C**). (**J**) LC-MS analysis of iminoctadine uptake in WT or *hol1Δ* pellets. Cells were treated with 1 µg/mL iminoctadine. Other experiment details are identical to those described for ATI-2307 in (**F**). (**K**) Mutations identified in Hol1 from 16 *spe1Δ hol1Δ* p[*HOL1*] strains exhibiting a separation-of-function phenotype. For each strain, all the mutations identified in Hol1 are listed, including synonymous mutations. Non-synonymous mutations shown in red were considered causal of the separation-of-function phenotype. For plasmids bearing multiple non-synonymous mutations in Hol1, the causal mutation was assigned to mutations identified in several independent plasmids, e.g., N57 and E327. (**L**) AlphaFold2 model of the *S. cerevisiae* Hol1 protein (UniProt Identifier P53389) showing the positions of the amino acid residues that were considered causal of the separation-of-function phenotype when mutated.

The online version of this article includes the following source data and figure supplement(s) for figure 4:

Source data 1. Source data for the plot of ***Figure 4C***.

Source data 2. Source data for the plot of ***Figure 4E***.

Source data 3. Source data for the plot of ***Figure 4F,H and J***.

Source data 4. Source data for the plot of ***Figure 4G***.

Source data 5. Source data for the plot of ***Figure 4I***.

Figure supplement 1. Chemical structures of (A) ATI-2307, (B) pentamidine, (C) spermidine, and (D) iminoctadine.

Figure supplement 2. Chromatograms and mass spectra for (**A**) yeast lysate spiked with 1.25 µg/mL ATI-2307, (**B**) lysate obtained from ATI-2307-treated wild-type (WT) sample, and (**C**) lysate obtained from ATI-2307-treated *hol1Δ* sample.

Figure supplement 3. Chromatograms and mass spectra for (**A**) yeast lysate spiked with 1.25 µg/mL pentamidine, (**B**) lysate obtained from pentamidine-treated wild-type (WT) sample (diluted 1/10 in yeast lysate), and (**C**) lysate obtained from pentamidine-treated *hol1Δ* sample.

Figure supplement 4. Chromatograms and mass spectra for (**A**) yeast lysate spiked with 1.25 µg/mL iminoctadine, (**B**) lysate obtained from iminoctadine-treated wild-type (WT) sample (diluted 1/10 in yeast lysate), and (**C**) lysate obtained from iminoctadine-treated *hol1Δ* sample.

Figure supplement 5. Streaks of *spe1Δ* and *spe1Δ hol1Δ* strains on SC 2% ethanol medium supplemented with 1 µM spermidine.

Figure supplement 6. Disc diffusion assays testing ATI-2307, pentamidine, and iminoctadine susceptibility of separation-of-function Hol1 mutants.

ATI-2307 susceptibility. Hol1 was recently identified as a high-affinity polyamine transporter in *S. cerevisiae* (***Vindu et al., 2021***). Strikingly, ATI-2307 uptake by *C. albicans* depends on the activity of an unidentified polyamine transporter (***Nishikawa et al., 2010***; ***Nishikawa et al., 2016***). Together, this suggested that Hol1 might be the transporter responsible for ATI-2307 uptake. Consistently, the deletion of *HOL1* confers ATI-2307 resistance, increasing the minimal inhibitory concentration 1000-fold from 0.001 to 1 µg/mL (***Figure 4C***). Moreover, Hol1 transport is driven by the plasma membrane proton-motive force (PMF) (***Vindu et al., 2021***), and transposon insertions predicted to weaken the PMF were positively selected by ATI-2307. This included insertions in the CDSs of *PTK2* and *PSG1* (***Figure 4A***, blue), both of which positively regulate the H^+-ATPase Pma1 (***Eraso et al., 2006***; ***Geva et al., 2017***; ***Goossens et al., 2000***), which generates the PMF (***Serrano et al., 1986***). ATI-2307 also positively selected transposons mapping to the extreme 3′-end of *TRK1* (***Figure 4D***, blue arrowhead). The deletion of the last 35 amino acids of Trk1 increases the stability of the Trk1-Trk2 potassium ion transporter (***Pérez-Valle et al., 2007***), which dissipates the PMF (***Gaber et al., 1988***; ***Ko et al., 1990***; ***Madrid et al., 1998***). There was also a significant enrichment of transposons in the promoters of

HAL4 and *HAL5* (**Figure 4D**, red arrowheads), two partially redundant positive regulators of Trk1-Trk2, and in the CDS of *SKY1* (**Figure 4A**, blue), a negative regulator of Trk1-Trk2 (**Mulet et al., 1999**; **Pérez-Valle et al., 2007**; **Forment et al., 2002**). Like *ptk2Δ* mutants, *sky1Δ* mutants are resistant to toxic concentrations of ATI-2307 (**Nishikawa et al., 2016**) and polyamines (**Erez and Kahana, 2001**; **Forment et al., 2002**; **Kaouass et al., 1997**).

ATI-2307 accumulates to high concentrations inside *C. albicans* cells (**Nishikawa et al., 2010**). We reasoned that if the same was true in *S. cerevisiae*, lysate from ATI-2307-treated WT cells may contain enough ATI-2307 to inhibit the growth of another *S. cerevisiae* culture, and that this might depend on Hol1. We treated non-fermentative WT and *hol1Δ* cultures in log-phase with an inhibitory concentration of ATI-2307 (0.003 µg/mL) for 2 hr. Cells were then harvested, washed, and homogenised. Lysate from ATI-2307-treated WT cells inhibited the growth of non-fermentative WT cultures, but not *hol1Δ* cultures (**Figure 4E**, left), indicating that the growth inhibition was indeed due to ATI-2307. In contrast, lysate from ATI-2307-treated *hol1Δ* cells lacked inhibitory activity (**Figure 4E**, right), consistent with Hol1-dependent ATI-2307 accumulation in *S. cerevisiae*. Liquid chromatography-mass spectrometry (LC-MS) was then used to quantify Hol1-dependent ATI-2307 accumulation in WT and *hol1Δ* cells. Whilst an average of 0.1 µg ATI-2307 was detected per gram of WT pellet, the concentration in *hol1Δ* lysates was below the detection limit (i.e. less than ~0.005 µg/mL) (**Figure 4F**). Thus, Hol1 is responsible for the selective accumulation of ATI-2307 in *S. cerevisiae*. Moreover, the heterologous expression of *C. albicans HOL1* (*CaHOL1*) partially restored ATI-2307 uptake (**Figure 4F**) and sensitivity (**Figure 4C**) in the *hol1Δ* mutants, indicating that Hol1 also imports ATI-2307 into fungal pathogens.

Pentamidine is an antiprotozoal drug that shares a similar chemical structure to ATI-2307 (**Figure 4—figure supplement 1**). Given that pentamidine competitively inhibits the uptake of polyamines and ATI-2307 by *C. albicans* (**Nishikawa et al., 2010**; **Nishikawa et al., 2016**), we hypothesised that Hol1 also imports pentamidine. Consistent with this, *hol1Δ* mutants showed reduced pentamidine susceptibility (**Figure 4G**) and uptake (**Figure 4H**), and pentamidine susceptibility was partially restored by the heterologous expression of *CaHOL1* (**Figure 4G**). Additionally, we assessed whether Hol1 imports iminoctadine (**Figure 4—figure supplement 1**), a polyamine found within the fungicide guazatine (**Castagnolo et al., 2011**) that has activity against multiple fungal phytopathogens (**Ryu et al., 2014**; **Zhu et al., 2019**) and fluconazole-resistant *Candida* spp. (**Castagnolo et al., 2011**). As shown in **Figure 4I**, iminoctadine susceptibility was reduced by the deletion of *HOL1*, which could be reversed by *CaHOL1* expression. Consistently, WT and *hol1Δ* cells treated for 2 hr with 1 µg/mL iminoctadine showed a striking 3500-fold difference in iminoctadine uptake (52.5 µg per gram of WT pellet versus 0.015 µg per gram of *hol1Δ* pellet) (**Figure 4J**). These results demonstrate that Hol1 also imports pentamidine and iminoctadine.

Our results indicate that loss-of-function mutations in Hol1 could confer ATI-2307 resistance in the clinic. However, the complete loss of this polyamine transporter is likely to carry a high fitness cost in low-nitrogen conditions (**Vindu et al., 2021**). This fitness cost might be circumvented by point mutations in *HOL1* that prevent ATI-2307 uptake while preserving polyamine import. Such separation-of-function mutations could present a caveat for the continued therapeutic development of ATI-2307. To assess whether separation-of-function mutations can arise, we performed a forward genetics screen that coupled random PCR mutagenesis to phenotypic screening. The principle underpinning the screen is that *HOL1* is essential for the growth of the polyamine auxotrophic *spe1Δ* strain in low-polyamine conditions (e.g. SC 2% ethanol +1 µM spermidine, **Figure 4—figure supplement 5**), but not in rich medium (**Fonzi, 1989**; **Whitney and Morris, 1978**). A plasmid library of randomly mutagenized *HOL1* genes was generated by gap-repair cloning in a *spe1Δ hol1Δ* strain. Approximately 10,000 transformants were then replica plated onto SC 2% ethanol medium containing 0.01 µg/mL ATI-2307 and 1 µM spermidine. Sixteen transformants showing ATI-2307 resistance were isolated before the plasmids were rescued. Seven plasmids were transformed back into the *spe1Δ hol1Δ* strain and disc diffusion assays confirmed resistance to ATI-2307, pentamidine, and iminoctadine (**Figure 4—figure supplement 6**). Given that *HOL1* is essential for *spe1Δ* strains on SC 2% ethanol (**Figure 4—figure supplement 5**), the resistance phenotypes confirmed that the *HOL1* alleles allowed spermidine uptake but limited import of ATI-2307, pentamidine, and iminoctadine. These results indicate that the transport activities of Hol1 can be functionally separated. All 16 plasmids were sequenced and contained at least one non-synonymous mutation in *HOL1* (**Figure 4K**). Furthermore, the codons for N57, L325, and E327 were mutated in more than one independent plasmid, suggesting that our

screen was approaching saturation. Mapping the mutated residues onto the AlphaFold2 model of Hol1 (***Jumper et al., 2021***) showed that most of these mutations clustered on the cytoplasmic side of Hol1 near the base of the pore (***Figure 4L***). This clustering suggests that our screen did not merely identify partial loss-of-function mutations in *HOL1*, but instead pinpointed a specific domain critical in mediating ATI-2307 uptake. Therefore, Hol1 mutations can disrupt its antifungal transport function without sacrificing its ability to transport polyamines, potentially allowing antifungal resistance to develop with minimal fitness cost.

Discussion

SATAY can accelerate the discovery of antifungal resistance mechanisms and modes of action

The rapid emergence of multidrug-resistant fungal pathogens is undermining our ability to control fungal infections. This problem is exacerbated by our incomplete understanding of the molecular mechanisms governing antifungal resistance and our limited armamentarium of antifungal compounds. Here, SATAY is applied to reveal loss- and gain-of-function mutations conferring resistance and sensitivity to 20 different antifungal compounds. These mutations pinpoint antifungal drug targets, transporters responsible for drug uptake or drug efflux, as well as metabolic, signalling and trafficking pathways affecting antifungal susceptibility. This study therefore provides a comprehensive dataset of cellular mechanisms that buffer fungal cells against diverse chemical stresses, which could inform the design of combination therapies and resistance management strategies. Moreover, by performing SATAY in PDR-attenuated strains, strains heterologously expressing drug targets and non-conventional strains, we identify resistance mechanisms and targets for compounds that lack activity against conventional laboratory strains of *S. cerevisiae*. SATAY therefore augments the range of antifungals amenable for screening with *S. cerevisiae*, creating opportunities for determining how resistance emerges against a broader spectrum of compounds.

Chitosan electrostatically interacts with mannosylphosphate on fungal cell surfaces

Chitosan is a natural antifungal compound with several attractive qualities, including biocompatibility, biodegradability, and non-toxicity. However, its application is constrained by the fact acidic conditions are required for solubility. Efforts are underway to create chitosan derivatives that improve bioavailability while preserving antifungal efficacy (***Hu and Luo, 2016***; ***Verlee et al., 2017***). One key challenge in these efforts is our lack of detailed knowledge regarding chitosan's specific molecular targets in fungi (***Qin and Li, 2020***). This gap has persisted partly because widely employed laboratory strains of *S. cerevisiae* such as S288C, which are used in conventional chemogenomic screening approaches, have minimal sensitivity to chitosan. Here, we perform SATAY in the chitosan-sensitive strain AD1-8, derived from the non-conventional strain US50-18C (***Decottignies et al., 1998***), and uncover mannosylphosphate as the cell wall target for chitosan. This finding may guide the development of chitosan derivatives with improved solubility and antifungal activity.

Interestingly, S288C-derived strains lacked cell wall mannosylphosphate, even though they harbour wild-type copies of *MNN4* and *MNN6*. The genetic determinants underpinning chitosan resistance in S288C-derived strains are multi-factorial, since upon crossing AD1-8 to ByK352 (an S288C-derived strain), we observed that chitosan sensitivity and alcian blue staining were inherited in a polygenic fashion (data not shown). The cell surfaces of S288C-derived strains have been modified by decades of selection in laboratory environments. For instance, S288C strains were deliberately selected to be defective in flocculation (***Mortimer and Johnston, 1986***), a process leading to unwanted cellular aggregations (***Stratford, 1992***). This is notable because mannan chains on the yeast cell wall are required for flocculation (***Stratford, 1992***). It seems possible that yeast geneticists have inadvertently selected for other mutations that affected cell wall mannosylphosphate. Additional basic traits for fungal pathogenicity, such as pseudo-hyphal growth (***Gancedo, 2001***) and biofilm formation (***Bojsen et al., 2012***), might have been accidentally or purposely lost from *S. cerevisiae* laboratory strains. SATAY therefore offers a unique opportunity for screening compounds targeting such processes in non-deficient, wild strains.

Hol1 imports ATI-2307, pentamidine, and iminoctadine into *S. cerevisiae*

We have identified that Hol1 is the high-affinity polyamine transporter responsible for the uptake and accumulation of ATI-2307, pentamidine, and iminoctadine in *S. cerevisiae*. Previous studies have reported that ATI-2307 has broad-spectrum activity against clinically significant *Candida* species, including *C. albicans*, *C. glabrata*, *C. parapsilosis*, *C. tropicalis*, and *C. auris* (***Mitsuyama et al., 2008***; ***Wiederhold et al., 2020***). Given that Hol1 from *C. albicans* can import ATI-2307 and that Hol1 is highly conserved across *Candida* species (64–78% pairwise amino acid sequence identity among the four species examined), it seems plausible that Hol1 orthologs across the *Candida* clade import ATI-2307.

Although carrier-mediated import of antifungal compounds has been described previously (***Galocha et al., 2020***; ***Lanthaler et al., 2011***), the propensity of Hol1 to concentrate ATI-2307 is unique and underpins the potency of this novel antifungal against yeasts. Few studies have investigated drug uptake by fungal pathogens (***Galocha et al., 2020***), yet they might harbour broad-spectrum, high-affinity nutrient permeases that could be hijacked by novel antifungal compounds. Identifying and characterising such transporters could be a promising strategy for bolstering antifungal development pipelines. The promiscuity of Hol1, with only loose structural homology between its identified substrates (***Figure 4—figure supplement 1***), makes it a promising candidate for the development of actively imported drugs or pro-drugs.

However, our study also reveals a straightforward pathway for the emergence of ATI-2307 resistance. While Hol1 is essential for polyamine uptake (***Vindu et al., 2021***), the single point mutations that we identified, which limit ATI-2307 uptake without perturbing polyamine uptake, could confer ATI-2307 resistance with little fitness cost. Gradual accumulation of additional mutations through sustained selection in the clinic might reduce any remaining costs. Therefore, by demonstrating that there exists a straightforward pathway for ATI-2307 resistance to arise, our findings may support further precautionary measures in the clinical use of ATI-2307.

Materials and methods

Yeast strains and culture conditions

S. cerevisiae strains and primers are listed in ***Supplementary files 4 and 5***, respectively. Gene deletions were generated by PCR-mediated gene disruption with selectable markers using the Longtine and Janke toolboxes (***Janke et al., 2004***; ***Longtine et al., 1998***). Yeast transformations were performed using lithium acetate (***Gietz and Schiestl, 2007***). Yeast strains yBL152 (ByK831, W303-1B), 12geneΔ0HSR (ByK1151), AD12345678 (ByK1174), BY4743Δ8a (ByK1230), and ABC16 Monster (ByK1266) were received as kind gifts from Prof. Mattias Peter (ETH Zurich), Prof. Françoise Strutz (University of Geneva), Prof. Mohan Gupta (University of Iowa), Prof. Martin Spiess (University of Basel), Prof. Frederick Roth (University of Toronto), respectively.

Synthetic media were made using either recipe A: 6.8 g/L yeast nitrogen base without amino acids (BD Difco, 291920), carbon source (glucose, galactose, raffinose, or ethanol) 2%, 1× amino acid mix (100× recipe: L-isoleucine [Sigma-Aldrich, W527602] 6 g/L, adenine hemisulfate salt [Sigma-Aldrich, A9126] 5.5 g/L, L-arginine [Thermo Fisher Scientific, A15738] 2 g/L, L-histidine monohydrochloride monohydrate [Sigma-Aldrich, H8000] 1 g/L, L-leucine [Sigma-Aldrich, L8000] 6 g/L, L-lysine monohydrochloride [Sigma-Aldrich, L8662] 4 g/L, L-methionine [Sigma-Aldrich, M9625] 1 g/L, L-phenylalanine [Sigma-Aldrich, P2126] 6 g/L, L-threonine [Sigma-Aldrich, 89179] 5 g/L, L-tryptophan [Sigma Aldrich, T0254] 4 g/L, L-tyrosine [Sigma-Aldrich, 93829] 5.5 g/L, uracil [Sigma-Aldrich, U1128] 5.5 g/L) recipe B: 1.7 g/L yeast nitrogen base without ammonium sulfate without amino acids (BD Difco, 233520), 5 g/L ammonium sulfate (Sigma, A4418), carbon source (glucose, galactose, raffinose, or ethanol) 2%, 1× amino acid mix (10× recipe: L-isoleucine [Sigma-Aldrich, W527602] 0.3 g/L, L-valine [Sigma-Aldrich, V0500] 1.5 g/L, adenine hemisulfate salt [Sigma-Aldrich, A9126] 0.4 g/L, L-arginine [Thermo Fisher Scientific, A15738] 0.2 g/L, L-histidine [Sigma-Aldrich, H8000] 0.2 g/L, L-leucine [Sigma-Aldrich, L8000] 1 g/L, L-lysine monohydrochloride [Sigma-Aldrich, L8662] 0.3 g/L, L-methionine [Sigma-Aldrich, M9625] 0.2 g/L, L-phenylalanine [Sigma-Aldrich, P2126] 0.5 g/L, L-threonine [Sigma-Aldrich, 89179] 2 g/L, L-tryptophan [Sigma Aldrich, T0254] 0.4 g/L, L-tyrosine [Sigma-Aldrich, 93829] 0.3 g/L, uracil [Sigma-Aldrich, U1128] 0.2 g/L, L-glutamic acid [Sigma-Aldrich, G1251] 1 g/L, L-aspartic acid [Thermo Fisher Scientific, A13520] 1 g/L) or recipe C: 1.7 g/L yeast nitrogen base without ammonium sulfate

without amino acids (BD Difco, 233520), 5 g/L ammonium sulfate (Sigma, A4418), carbon source (glucose, galactose, raffinose, or ethanol) 2%, 1× amino acid mix (10× recipe: L-isoleucine [Sigma-Aldrich, I2752] 0.3 g/L, L-valine [Carl Roth, 4879.3] 1.5 g/L, adenine hemisulfate salt [Sigma-Aldrich, A9126] 0.4 g/L, L-arginine monohydrochloride [Sigma-Aldrich, A5131] 0.2 g/L, L-histidine monohydrochloride monohydrate [Sigma-Aldrich, H8125] 0.2 g/L, L-leucine [Sigma-Aldrich, L8000] 1 g/L, L-lysine monohydrochloride [Sigma-Aldrich, L5626] 0.3 g/L, L-methionine [Sigma-Aldrich, M9625] 0.2 g/L, L-phenylalanine [Sigma-Aldrich, P2126] 0.5 g/L, L-threonine [Sigma-Aldrich, T8625] 2 g/L, L-tryptophan [Sigma-Aldrich, T0254] 0.4 g/L, L-tyrosine [Sigma-Aldrich, T3754] 0.3 g/L, uracil [Sigma-Aldrich, U0750] 0.2 g/L, L-glutamic acid monosodium salt hydrate [Sigma-Aldrich, G1626] 1 g/L, L-aspartic acid sodium salt monohydrate [Sigma-Aldrich, 11195] 1 g/L).

Specific components were excluded for the preparation of drop-out media.

YPD medium: Yeast extract (Appleton Woods Ltd, DM832) 11 g/L, peptone (BD Difco, 211677) 22 g/L, adenine hemisulfate salt (Sigma-Aldrich, A9126) 55 mg/L, glucose 2%. YPA medium: yeast extract (Appleton Woods Ltd, DM832) 10 g/L, peptone (BD Difco, 211677) 20 g/L, potassium acetate (Sigma-Aldrich, W292001) 10 g/L.

All cultures were incubated at 30°C, 200 rpm.

Plasmids

Plasmids are listed in ***Supplementary file 6***. Restriction enzymes were purchased from NEB.

To construct the plasmid p405-*TEF1*pr-*BdDRK1* (pBK864), the *DRK1* CDS from *B. dermatitidis* (NCBI Reference Sequence: EGE84246.1) was commercially synthesised with yeast codon optimisation, 5′ restriction site for *Spe*I and 3′ restriction site for *Pst*I (Biomatik, Canada). The *BdDRK1* CDS was then sub-cloned into p405-*TEF1*pr (Addgene plasmid #15968) using *Spe*I and *Pst*I and T4 DNA ligase (Thermo Fisher Scientific #EL0011).

The plasmid bearing the *HOL1* CDS from *C. albicans* (pBK994) was generated by gap-repair cloning. Briefly, the *CaHOL1* CDS was PCR-amplified from genomic DNA derived from *C. albicans* strain ATCC MYA-2876 using primers 11 and 12 (***Supplementary file 5***). The 5′ and 3′ ends of the *CaHOL1* PCR product were homologous to the *ScHOL1* 5′ UTR and 3′ UTR sequences on pBK958. The *ScHOL1* CDS was excised from pBK958 using *Bsu36*I and *Nru*I. The linearised pBK958 backbone was co-transformed with the *CaHOL1* PCR product into *hol1Δ* strain of *S. cerevisiae* (ByK2032). Plasmid pBK994 was verified by colony PCR.

Antifungal compounds

Antifungal compounds are listed in ***Supplementary file 2***. Compounds were stored at the manufacturer's recommended temperature. Stocks were prepared using dimethyl sulfoxide (DMSO) (Thermo Fisher Scientific, 10103483) or Milli-Q and stored at –20°C for maximally 18 months.

Chitosan preparation

Stocks of medium molecular weight chitosan (190–310 kDa, 75–85% deacetylated, shrimp shells) (Sigma-Aldrich, 448877) were prepared by nitrous deamination, as described previously (***Zakrzewska et al., 2005***). Briefly, 10 g chitosan was dissolved in 200 mL 10% acetic acid (Sigma-Aldrich, A6283) and incubated with 200 mg sodium nitrite (Sigma-Aldrich, 237213) in the dark at room temperature for 17 hr. The reaction was terminated by adjusting to pH 5.5 with 5 M NaOH.

Antifungal susceptibility tests

Bioscreen C

Sub-lethal concentrations of antifungal compounds were determined using a Bioscreen C instrument (Oy Growth Curves Ab Ltd, Helsinki, Finland). Cells were cultured from OD_{600} 0.2 in SC 2% glucose medium containing antifungal compounds at 30°C for 24 hr with continuous shaking, and OD_{600} readings were recorded every 20 min. Final DMSO concentrations in the cultures never exceeded 1% (vol/vol).

ATI-2307, pentamidine, and iminoctadine susceptibility tests

Yeast strains grown to saturation in SC-URA 2% ethanol 0.2% glucose were reseeded at OD_{600} 0.2 in SC-URA 2% ethanol containing ATI-2307, pentamidine, or iminoctadine. Wild-type strains were

transformed with an empty CEN/*URA3* plasmid (pRS316) (***Sikorski and Hieter, 1989***) whilst *hol1Δ* strains were transformed with pRS316 or plasmid pBK994, encoding *HOL1* from *C. albicans*.

Saturated transposon analysis in yeast

Library generation on SC-ADE 2% galactose plates

Transposon libraries were generated on SC-ADE 2% galactose plates using previously described protocols (***Michel et al., 2017***; ***Michel and Kornmann, 2022***), with the following modifications. First, the OD_{600} at plating for strains 12geneΔ0HSR *ade2Δ* (ByK1261) and AD12345678 *ade2Δ* (ByK1262) was 65 and 160, respectively. Second, the AD12345678 *ade2Δ* transposon library was harvested 10 days after transposition induction. Third, transposon libraries were not expanded in SC-ADE 2% glucose after harvest.

Library generation in liquid media

The culture volumes and media used for the generation of transposon libraries in liquid medium are summarised in ***Supplementary file 7***. Yeast strains were transformed with either pBK549 or pBK626. Individual pBK549 transformants were streaked on SC-URA 2% glucose and SC-ADE 2% glucose plates. Transformants that showed full growth on SC-URA whilst producing only a few colonies (2–6) on SC-ADE were scraped from the SC-URA plates and used to inoculate pre-cultures of SC-URA 2% raffinose and 0.2% glucose at OD_{600} 0.2 and grown to saturation. To induce transposition, saturated pre-cultures were diluted to OD_{600} 0.2 in SC-URA 2% galactose and grown for ~50 hr at 30°C, 200 rpm. Transposed cells were then diluted in SC-ADE 2% glucose and grown for ~70 hr to OD_{600}~2. Dilutions of transposed cultures were plated at T_0, T_{20} and at the end of induction on SC, SC-URA, and SC-ADE plates. Plating at T_0 served to estimate the background of ADE+ clones due to spontaneous recombination of pBK549 (typically 0.01% in BY4741 background and 0.007% in W303 background). Plating at T_{20} guided the re-inoculation following transposition. The number of ADE+ cells at T_{20} typically corresponds to ~10% of the number of ADE+ cells at the end of induction.

The protocol for generating transposon libraries with pBK626 transformants included the following modifications. First, individual pBK626 transformants were streaked on SC-URA 2% glucose and SC-TRP 2% glucose. Second, dilutions of induced cultures were plated at T_0, T_{20} and ~T_{50} on SC, SC-URA, and SC-TRP plates. Third, following transposition, cells were diluted in SC-TRP 2% glucose at OD_{600} 1 and grown to saturation, before a second re-growth was performed in SC-TRP 2% glucose from OD_{600} 0.3 to saturation. Fourth, cells were pelleted and stored at –80°C as 30% (vol/vol) glycerol stocks.

Prior to ATI-2307 treatment, the ByK831 transposon library was thawed from –80°C glycerol stock and grown from OD_{600} 0.25 to saturation in 1.2 L of SC-TRP 2% glucose.

Antifungal compound treatments of transposon libraries

Transposon libraries were treated for two successive growth rounds from OD_{600} 0.1–0.2 to saturation (OD_{600}~5) at 30°C, 200 rpm in the presence of antifungal compounds at the concentrations indicated in ***Supplementary file 2***, in media and volumes summarised in ***Supplementary file 8***. Cultures were harvested for cell pellets after the second growth round, using previously described protocols (***Michel et al., 2017***; ***Michel and Kornmann, 2022***) and stored at –80°C.

The first treatments with amphotericin B (0.75 µg/mL) and caspofungin (0.03 µg/mL) initially prevented growth. These cultures were diluted 2× in fresh medium after 24 hr. The first oxytriazine treatment (1.491 µg/mL) prevented growth so culture was diluted 3× in fresh medium after 46 hr.

Prior to ATI-2307 treatment in SC-TRP 2% ethanol, the ByK831 transposon library was adapted to respiratory conditions by growing to saturation in 500 mL SC-TRP 2% ethanol 0.2% glucose medium.

Transposon library sequencing and bioinformatics analysis

Cell pellets were processed for sequencing following previously described protocols (***Michel et al., 2017***; ***Michel and Kornmann, 2022***). Barcoded transposon libraries were pooled and sequenced using the NextSeq 500/550 High Output Kit v2.5 (75 cycles) (Illumina, 20024906) and NextSeq 500 Sequencing System (Illumina, SY-415-1001) following the manufacturer's guidelines. Bioinformatics analysis of SATAY sequencing data was performed as described in ***Michel et al., 2017***; ***Michel and***

Kornmann, 2022. The *.bed* and *.wig* output files were uploaded to UCSC Genome Browser to visualise transposition events and read counts per transposon, respectively.

GO term analyses

GO term analyses were performed using GO Term Finder (v0.86) (https://www.yeastgenome.org/) for the 25–50 genes with the highest read counts (or the lowest number of transposons) in the compound treatment relative to the control treatment. The background set of genes consisted of all the 6603 genes in the *S. cerevisiae* genome. Holm-Bonferroni-corrected GO term enrichments were computed for the 'Process' Ontology aspect with a p-value below 0.01.

Alcian blue dye binding assay

Saturated yeast grown in SC 2% glucose were treated with 10 µg/mL Alcian blue solution (Sigma-Aldrich, 1016470500) at room temperature for 3 min after brief vortexing. Cells were then centrifuged before the pellets were imaged.

Live imaging of yeast

Yeast grown to saturation in SC 2% glucose medium were treated with 25 µg/mL fluorescein-labelled chitosan (CD Bioparticles, CDHA061) for 2 hr. For the last 30 min of the fluorescein-labelled chitosan treatment, cells were optionally treated with 0.1 µM MitoTracker Orange CMTMRos (Thermo Fisher Scientific, M7510). Cells were then washed twice and mixed pairwise, transferred to the microscope slide and imaged using an IX81 Olympus inverted spinning disk microscope with an EM-CCD camera (Hamamatsu Photonics) using a 100× oil objective (NA = 1.4). Images were analysed using ImageJ (v1.53c).

Assessing ATI-2307, pentamidine, and iminoctadine accumulation in *S. cerevisiae*

Generating cell lysate

Wild-type and *hol1Δ* strains were grown to saturation in SC 2% ethanol 0.2% glucose. Cells were then reseeded at OD_{600} 0.5 in SC 2% ethanol (1 L for subsequent cell lysate treatments; 200 mL for subsequent LC-MS experiments), and upon reaching OD_{600}~1, the cells were treated with ATI-2307 (0.003 µg/mL), pentamidine (1 µg/mL), or iminoctadine (1 µg/mL) for 2 hr. Cultures were harvested by centrifugation before cell pellets were washed three times in SC 2% ethanol.

For subsequent yeast growth inhibition, cell lysate was obtained by resuspending ~500 mg cell pellets in 500 µL Cell Breaking Buffer (2% Triton X-100, 1% SDS, 100 mM NaCl, 100 mM Tris-HCl, pH 8.0, 1 mM EDTA). Cell suspensions were distributed into 280 µL aliquots, to which 400 µL SC 2% ethanol and 200 µL 0.5 mm Glass Mill Beads (BioSpec Products, 11079105) were added, before vortexing at 2850 rpm for 10 min, 4°C, using a Disruptor Genie (Scientific Industries, SI-DD38). Aliquots were centrifuged before the lysate was collected.

For LC-MS, ~500 mg cell pellets were resuspended in 500 µL 80% (vol/vol) acetonitrile (HPLC-grade, VWR) 20% (vol/vol) Milli-Q and stored at –20°C for ~24 hr. Cell suspensions were then transferred to 2 mL tubes (Precellys MK28-R Hard Tissue Grinding Kit, Bertin Technologies), from which the steel beads were replaced with 200 µL 0.5 mm Glass Mill Beads (BioSpec Products, 11079105). Bead-beating was performed using a Precellys Evolution homogeniser (Bertin Technologies, P002511-PEVT0-A.0) at 6000 rpm for 10 cycles of: 1 min beating, 30 s pause, 1 min beating. Cycles were spaced by 2 min intervals, during which the samples were kept on ice. Samples were centrifuged before the lysates were collected and stored at –20°C until LC-MS analysis.

Cell lysate treatments

Yeast grown to saturation in SC 2% ethanol 0.2% glucose were reseeded at OD_{600} 0.2 in 10 mL SC 2% ethanol and treated with 64 µL lysate.

LC-MS analysis

LC-MS analysis was performed using a Vanquish Flex Tandem UHPLC system (Thermo Fisher Scientific, UK) connected to a Q-Exactive Hybrid Quadrupole-Orbitrap Mass Spectrometer (Thermo Fisher

Scientific, UK). Samples were injected at a volume of 5 µL and separated using one of two ACQUITY Premier BEH C18 Columns with VanGuard FIT, 1.7 µm, 2.1×50 mm (Waters, 186009455) at a column temperature of 40°C and a flow rate of 700 µL/min. Samples were analysed using a 6 min gradient method using water with 0.2% (vol/vol) formic acid (Optima LC/MS-grade, Thermo Fisher Scientific, UK) and acetonitrile (HPLC-grade, VWR) as the A and B mobile phases, respectively. Starting with 95% mobile phase A, 5% mobile phase B, the LC gradient was as follows: 0.0→1.0 min (5% B), 1.0→2.0 min (5%→95% B), 2.0→5.0 min (95% B), 5.0→5.1 min (95%→5% B), 5.1→6.0 min (5% B). Flow from the column was sent to the mass spectrometer in a window set to between 0.5 and 4.5 min. Three consecutive injections of acetonitrile/water (80/20 [vol/vol]) were performed after each sample injection to prevent carry-over.

Mass spectrometry analysis was performed with electrospray ionisation in positive ionisation mode using the following source conditions: source gas flow = 55 arb. units; auxiliary gas flow = 10 arb. units; auxiliary gas heater; temperature = 310°C; spray voltage = 3.2 kV; capillary temperature = 320°C; S-lens RF level = 55.0 arb. units. Analysis was performed using a full scan MS method with 35,000 mass resolution at 200 *m/z*, and a scan window from 100 to 900 *m/z*. Target peaks were as follows: ATI-2307 *m/z*=219.6468 $[M+2H]^{2+}$, iminoctadine *m/z*=178.6784 $[M+2H]^{2+}$, pentamidine *m/z*=171.1022 $[M+2H]^{2+}$.

Sample quantifications of ATI-2307, iminoctadine, and pentamidine were performed using matrix-matched calibration curves with R^2 values greater than 0.996. Calibration curves were prepared using serial dilutions of compound stock solutions in yeast lysate extracts. For pentamidine and iminoctadine, two calibration curves were prepared: one to quantify the wild-type samples and one to quantify the *hol1Δ* samples. Calibration curves were calculated using Xcalibur (Thermo Fisher Scientific, v4.6), and the *m/z* of the peaks for each calibration point were verified using Quan Browser software (Thermo Fisher Scientific, v4.6).

Screening for separation-of-function mutations in *HOL1*

The CEN/*URA3* plasmid bearing *S. cerevisiae HOL1* (pBK958), a kind gift from Dr. Thomas Dever (NIH, Bethesda, MD, USA), served as the template for PCR. The *ScHOL1* CDS and flanking UTR sequences were PCR-amplified using *Taq* DNA Polymerase, generating a product that contained 5′ and 3′ sequences homologous to the pBK958 backbone. *ScHOL1* CDS was excised from pBK958 using *Bsu36*I and *Age*I, and the resulting pBK958 backbone was co-transformed into the *spe1Δ hol1Δ* strain (ByK2037) with the *ScHOL1* PCR product. Transformants were selected on SC-URA 2% glucose, and subsequently replica plated onto SC-URA 2% ethanol medium containing 1 µM spermidine (Sigma-Aldrich, S2626) and 0.01 µg/mL ATI-2307. ATI-2307-resistant isolated colonies were then streaked onto SC-URA 2% ethanol + 1 µM spermidine + 0.01 µg/mL ATI-2307 plates for a second round of selection. Plasmids were isolated from ATI-2307-resistant colonies, sequenced, and re-transformed back into the *spe1Δ hol1Δ* strains prior to disc diffusion assays.

Disc diffusion assays

Cells were grown to saturation in 5 mL SC-URA 2% ethanol 0.2% glucose medium supplemented with 1 mM spermidine and 100 nM pantothenic acid. 175 µL of each saturated culture was then plated on SC 2% ethanol supplemented with 1 µM spermidine. Discs (Thermo Fisher Scientific, 10066142) were wetted with 17 µL of each drug (ATI-2307 0.4 µg/mL; pentamidine 80 µg/mL; iminoctadine 30 µg/mL) and placed on the agar surface. Plates were incubated at 30°C for 5 days before imaging.

Materials availability statement

Strains and plasmids are available upon request.

Acknowledgements

The authors are grateful to Christian Coville-Cooke and Ying-Chen Lin for feedback on the manuscript and technical support; Anitha Nair and Yaan Jang for technical support; Jack Rice for technical support and assistance with LC-MS. MTK was supported by an Industrial CASE (iCASE) Studentship, jointly funded by the BBSRC and Syngenta (grant number BB/T008784/1). The Kornmann Lab is funded by Wellcome Trust grant 214291/Z/18/Z.

Additional information

Funding

Funder	Grant reference number	Author
Biotechnology and Biological Sciences Research Council	BB/T008784/1	Matthew T Karadzas
Wellcome Trust	10.35802/214291	Agnès H Michel Benoit Kornmann

The funders had no role in study design, data collection and interpretation, or the decision to submit the work for publication. For the purpose of Open Access, the authors have applied a CC BY public copyright license to any Author Accepted Manuscript version arising from this submission.

Author contributions

Matthew T Karadzas, Conceptualization, Data curation, Formal analysis, Investigation, Visualization, Methodology, Writing – original draft, Writing – review and editing; Agnès H Michel, Resources, Data curation, Software, Formal analysis, Supervision, Investigation, Visualization, Methodology, Writing – review and editing; Andreas Mosbach, Investigation, Visualization, Writing – review and editing; George Giannakopoulos, Investigation, Visualization; Ruairi McGettigan, Investigation, Visualization, Methodology; Gabriel Scalliet, Conceptualization, Formal analysis, Supervision, Visualization, Methodology, Writing – review and editing; Benoit Kornmann, Conceptualization, Data curation, Software, Formal analysis, Supervision, Funding acquisition, Visualization, Writing – original draft, Project administration, Writing – review and editing

Author ORCIDs

Agnès H Michel https://orcid.org/0000-0001-9386-0170
Andreas Mosbach https://orcid.org/0009-0002-8319-9504
George Giannakopoulos https://orcid.org/0000-0001-9070-1473
Ruairi McGettigan https://orcid.org/0009-0002-8270-8848
Gabriel Scalliet https://orcid.org/0000-0002-7291-2522
Benoit Kornmann https://orcid.org/0000-0002-6030-8555

Peer review material

Version of Record:
Reviewer #1 (Public review): https://doi.org/10.7554/eLife.105333.2.sa1
Reviewer #2 (Public review): https://doi.org/10.7554/eLife.105333.2.sa2
Reviewer #3 (Public review): https://doi.org/10.7554/eLife.105333.2.sa3

Reviewed preprint v1
Reviewer #1 (Public review): https://doi.org/10.7554/eLife.105333.1.sa2
Reviewer #2 (Public review): https://doi.org/10.7554/eLife.105333.1.sa1
Reviewer #3 (Public review): https://doi.org/10.7554/eLife.105333.1.sa0
eLife Assessment https://doi.org/10.7554/eLife.105333.1.sa3

Additional files

Supplementary files

MDAR checklist

Supplementary file 1. List of screens performed in this study.

Supplementary file 2. Antifungal drugs used in this study.

Supplementary file 3. GO term analysis of the hits of the different screens of this study.

Supplementary file 4. List of yeast strains used in this study.

Supplementary file 5. List of oligonucleotides used in this study.

Supplementary file 6. List of plasmids used in this study.

Supplementary file 7. Culture volumes and media used for the generation of transposon libraries in liquid medium.

Supplementary file 8. Summary of library antifungal treatments performed in this study.

Supplementary file 9. Summary of the number of insertions and reads per genes in all libraries.

Data availability

All data supporting the findings of this study are available in the main text, supplementary materials, and associated data repositories. The raw SATAY sequencing data have been deposited in the European Nucleotide Archive (ENA) under study accession numbers PRJEB129441 and PRJEB35463. Processed transposon insertion data can be explored using the UCSC Genome Browser through two publicly accessible sessions: Transposon insertion maps: https://genome.ucsc.edu/s/Matthew%20Karadzas/Transposon_Maps_Karadzas_2024. Transposon insertion histograms: https://genome.ucsc.edu/s/Matthew%20Karadzas/Histograms_Karadzas%202024. Number of insertions and reads per genes in all libraries are found in the ***Supplementary file 9***.
The following datasets were generated: ***Karadzas et al., 2026a***, ***Karadzas et al., 2026b***

References

Alarco AM, Balan I, Talibi D, Mainville N, Raymond M. 1997. AP1-mediated multidrug resistance in *Saccharomyces cerevisiae* requires FLR1 encoding a transporter of the major facilitator superfamily. *The Journal of Biological Chemistry* **272**:19304–19313. DOI: https://doi.org/10.1074/jbc.272.31.19304, PMID: 9235926

Alepuz PM, de Nadal E, Zapater M, Ammerer G, Posas F. 2003. Osmostress-induced transcription by Hot1 depends on a Hog1-mediated recruitment of the RNA Pol II. *The EMBO Journal* **22**:2433–2442. DOI: https://doi.org/10.1093/emboj/cdg243, PMID: 12743037

Arya N, Rahman H, Rudrow A, Wagner M, Schmitt L, Ambudkar SV, Golin J. 2019. An A666G mutation in transmembrane helix 5 of the yeast multidrug transporter Pdr5 increases drug efflux by enhancing cooperativity between transport sites. *Molecular Microbiology* **112**:1131–1144. DOI: https://doi.org/10.1111/mmi.14351, PMID: 31294884

Ballou CE. 1990. Isolation, characterization, and properties of *Saccharomyces cerevisiae* MNN mutants with nonconditional protein glycosylation defects. *Methods in Enzymology* **185**:440–470. DOI: https://doi.org/10.1016/0076-6879(90)85038-P

Bautista-Baños S, Hernández-Lauzardo AN, Velázquez-del Valle MG, Hernández-López M, Ait Barka E, Bosquez-Molina E, Wilson CL. 2006. Chitosan as a potential natural compound to control pre and postharvest diseases of horticultural commodities. *Crop Protection* **25**:108–118. DOI: https://doi.org/10.1016/j.cropro.2005.03.010

Becher R, Wirsel SGR. 2012. Fungal cytochrome P450 sterol 14α-demethylase (CYP51) and azole resistance in plant and human pathogens. *Applied Microbiology and Biotechnology* **95**:825–840. DOI: https://doi.org/10.1007/s00253-012-4195-9, PMID: 22684327

Behnia R, Panic B, Whyte JRC, Munro S. 2004. Targeting of the Arf-like GTPase Arl3p to the Golgi requires N-terminal acetylation and the membrane protein Sys1p. *Nature Cell Biology* **6**:405–413. DOI: https://doi.org/10.1038/ncb1120, PMID: 15077113

Berninsone P, Miret JJ, Hirschberg CB. 1994. The Golgi guanosine diphosphatase is required for transport of GDP-mannose into the lumen of *Saccharomyces cerevisiae* Golgi vesicles. *The Journal of Biological Chemistry* **269**:207–211. DOI: https://doi.org/10.1016/s0021-92581742335-0, PMID: 7506254

Bojsen RK, Andersen KS, Regenberg B. 2012. *Saccharomyces cerevisiae*--a model to uncover molecular mechanisms for yeast biofilm biology. *FEMS Immunology and Medical Microbiology* **65**:169–182. DOI: https://doi.org/10.1111/j.1574-695X.2012.00943.x, PMID: 22332975

Bojsen R, Regenberg B, Gresham D, Folkesson A. 2016. A common mechanism involving the TORC1 pathway can lead to amphotericin B-persistence in biofilm and planktonic *Saccharomyces cerevisiae* populations. *Scientific Reports* **6**:21874. DOI: https://doi.org/10.1038/srep21874, PMID: 26903175

Bongomin F, Gago S, Oladele RO, Denning DW. 2017. Global and multi-national prevalence of fungal diseases-estimate precision. *Journal of Fungi* **3**:57. DOI: https://doi.org/10.3390/jof3040057, PMID: 29371573

Brandhorst TT, Kean IRL, Lawry SM, Wiesner DL, Klein BS. 2019. Phenylpyrrole fungicides act on triosephosphate isomerase to induce methylglyoxal stress and alter hybrid histidine kinase activity. *Scientific Reports* **9**:5047. DOI: https://doi.org/10.1038/s41598-019-41564-9, PMID: 30911085

Bruinsma P, Spelbrink RG, Nothwehr SF. 2004. Retrograde transport of the mannosyltransferase Och1p to the early Golgi requires a component of the COG transport complex. *The Journal of Biological Chemistry* **279**:39814–39823. DOI: https://doi.org/10.1074/jbc.M405500200, PMID: 15229219

Buschart A, Gremmer K, El-Mowafy M, van den Heuvel J, Mueller PP, Bilitewski U. 2012. A novel functional assay for fungal histidine kinases group III reveals the role of HAMP domains for fungicide sensitivity. *Journal of Biotechnology* **157**:268–277. DOI: https://doi.org/10.1016/j.jbiotec.2011.09.017, PMID: 21963586

Castagnolo D, Schenone S, Botta M. 2011. Guanylated diamines, triamines, and polyamines: chemistry and biological properties. *Chemical Reviews* **111**:5247–5300. DOI: https://doi.org/10.1021/cr100423x, PMID: 21657224

Catlett NL, Yoder OC, Turgeon BG. 2003. Whole-genome analysis of two-component signal transduction genes in fungal pathogens. *Eukaryotic Cell* **2**:1151–1161. DOI: https://doi.org/10.1128/EC.2.6.1151-1161.2003, PMID: 14665450

Chen P, Michel AH, Zhang J. 2022. Transposon insertional mutagenesis of diverse yeast strains suggests coordinated gene essentiality polymorphisms. *Nature Communications* **13**:1–15. DOI: https://doi.org/10.1038/s41467-022-29228-1

Chinen T, Ota Y, Nagumo Y, Masumoto H, Usui T. 2011. Construction of multidrug-sensitive yeast with high sporulation efficiency. *Bioscience, Biotechnology, and Biochemistry* **75**:1588–1593. DOI: https://doi.org/10.1271/bbb.110311, PMID: 21821930

Coe KA, Lee W, Stone MC, Komazin-Meredith G, Meredith TC, Grad YH, Walker S. 2019. Multi-strain Tn-Seq reveals common daptomycin resistance determinants in *Staphylococcus aureus*. *PLOS Pathogens* **15**:e1007862. DOI: https://doi.org/10.1371/journal.ppat.1007862, PMID: 31738809

Conaway RC, Conaway JW. 2009. The INO80 chromatin remodeling complex in transcription, replication and repair. *Trends in Biochemical Sciences* **34**:71–77. DOI: https://doi.org/10.1016/j.tibs.2008.10.010, PMID: 19062292

Daum G, Tuller G, Nemec T, Hrastnik C, Balliano G, Cattel L, Milla P, Rocco F, Conzelmann A, Vionnet C, Kelly DE, Kelly S, Schweizer E, Schüller HJ, Hojad U, Greiner E, Finger K. 1999. Systematic analysis of yeast strains with possible defects in lipid metabolism. *Yeast* **15**:601–614. DOI: https://doi.org/10.1002/(SICI)1097-0061(199905)15:7<601::AID-YEA390>3.0.CO;2-N

Decottignies A, Grant AM, Nichols JW, de Wet H, McIntosh DB, Goffeau A. 1998. ATPase and multidrug transport activities of the overexpressed yeast ABC protein Yor1p. *The Journal of Biological Chemistry* **273**:12612–12622. DOI: https://doi.org/10.1074/jbc.273.20.12612, PMID: 9575223

Demuyser L, Van Dijck P. 2019. Can *Saccharomyces cerevisiae* keep up as a model system in fungal azole susceptibility research? *Drug Resistance Updates* **42**:22–34. DOI: https://doi.org/10.1016/j.drup.2019.02.002, PMID: 30822675

Denning DW. 2024. Global incidence and mortality of severe fungal disease. *The Lancet. Infectious Diseases* **24**:e428–e438. DOI: https://doi.org/10.1016/S1473-3099(23)00692-8, PMID: 38224705

Duina AA, Miller ME, Keeney JB. 2014. Budding yeast for budding geneticists: a primer on the *Saccharomyces cerevisiae* model system. *Genetics* **197**:33–48. DOI: https://doi.org/10.1534/genetics.114.163188, PMID: 24807111

Edskes HK, Mukhamedova M, Edskes BK, Wickner RB. 2018. *Hermes* transposon mutagenesis shows [URE3] prion pathology prevented by a ubiquitin-targeting protein: evidence for carbon/nitrogen assimilation cross talk and a second function for Ure2p in *Saccharomyces cerevisiae*. *Genetics* **209**:789–800. DOI: https://doi.org/10.1534/genetics.118.300981, PMID: 29769283

Eraso P, Mazón MJ, Portillo F. 2006. Yeast protein kinase Ptk2 localizes at the plasma membrane and phosphorylates in vitro the C-terminal peptide of the H+-ATPase. *Biochimica et Biophysica Acta (BBA) - Biomembranes* **1758**:164–170. DOI: https://doi.org/10.1016/j.bbamem.2006.01.010

Erez O, Kahana C. 2001. Screening for modulators of spermine tolerance identifies Sky1, the SR protein kinase of *Saccharomyces cerevisiae*, as a regulator of polyamine transport and ion homeostasis. *Molecular and Cellular Biology* **21**:175–184. DOI: https://doi.org/10.1128/MCB.21.1.175-184.2001, PMID: 11113192

Fillinger S, Ajouz S, Nicot PC, Leroux P, Bardin M. 2012. Functional and structural comparison of pyrrolnitrin- and iprodione-induced modifications in the class III histidine-kinase Bos1 of Botrytis cinerea. *PLOS ONE* **7**:e42520. DOI: https://doi.org/10.1371/journal.pone.0042520, PMID: 22912706

Fisher MC, Hawkins NJ, Sanglard D, Gurr SJ. 2018. Worldwide emergence of resistance to antifungal drugs challenges human health and food security. *Science* **360**:739–742. DOI: https://doi.org/10.1126/science.aap7999, PMID: 29773744

Fones HN, Bebber DP, Chaloner TM, Kay WT, Steinberg G, Gurr SJ. 2020. Threats to global food security from emerging fungal and oomycete crop pathogens. *Nature Food* **1**:332–342. DOI: https://doi.org/10.1038/s43016-020-0075-0, PMID: 37128085

Fonzi WA. 1989. Biochemical and genetic characterization of the structure of yeast ornithine decarboxylase. *Biochemical and Biophysical Research Communications* **162**:1409–1416. DOI: https://doi.org/10.1016/0006-291X(89)90831-0

Forment J, Mulet JM, Vicente O, Serrano R. 2002. The yeast SR protein kinase Sky1p modulates salt tolerance, membrane potential and the Trk1,2 potassium transporter. *Biochimica et Biophysica Acta (BBA) - Biomembranes* **1565**:36–40. DOI: https://doi.org/10.1016/S0005-2736(02)00503-5

Fröhlich F, Petit C, Kory N, Christiano R, Hannibal-Bach HK, Graham M, Liu X, Ejsing CS, Farese RV, Walther TC. 2015. The GARP complex is required for cellular sphingolipid homeostasis. *eLife* **4**:e08712. DOI: https://doi.org/10.7554/eLife.08712, PMID: 26357016

Furukawa K, Randhawa A, Kaur H, Mondal AK, Hohmann S. 2012. Fungal fludioxonil sensitivity is diminished by a constitutively active form of the group III histidine kinase. *FEBS Letters* **586**:2417–2422. DOI: https://doi.org/10.1016/j.febslet.2012.05.057

Gaber RF, Styles CA, Fink GR. 1988. TRK1 encodes a plasma membrane protein required for high-affinity potassium transport in *Saccharomyces cerevisiae*. *Molecular and Cellular Biology* **8**:2848–2859. DOI: https://doi.org/10.1128/mcb.8.7.2848-2859.1988, PMID: 3043197

Gale AN, Sakhawala RM, Levitan A, Sharan R, Berman J, Timp W, Cunningham KW. 2020. Identification of essential genes and fluconazole susceptibility genes in *Candida glabrata* by profiling *Hermes* transposon

insertions. *G3: Genes, Genomes, Genetics* **10**:3859–3870. DOI: https://doi.org/10.1534/g3.120.401595, PMID: 32819971

Gale AN, Pavesic MW, Nickels TJ, Xu Z, Cormack BP, Cunningham KW. 2023. Pdr1 functions as a sensor of cellular stresses in Candida glabrata. *mSphere* **8**:e00254-23. DOI: https://doi.org/10.1128/msphere.00254-23

Gallagher LA, Shendure J, Manoil C. 2011. Genome-scale identification of resistance functions in *Pseudomonas aeruginosa* using Tn-seq. *mBio* **2**:e00315-10. DOI: https://doi.org/10.1128/mBio.00315-10, PMID: 21253457

Galocha M, Costa IV, Teixeira MC. 2020. Carrier-mediated drug uptake in fungal pathogens. *Genes* **11**:1324. DOI: https://doi.org/10.3390/genes11111324, PMID: 33182427

Galván Márquez I, Akuaku J, Cruz I, Cheetham J, Golshani A, Smith ML. 2013. Disruption of protein synthesis as antifungal mode of action by chitosan. *International Journal of Food Microbiology* **164**:108–112. DOI: https://doi.org/10.1016/j.ijfoodmicro.2013.03.025, PMID: 23624539

Gancedo JM. 2001. Control of pseudohyphae formation in *Saccharomyces cerevisiae*. *FEMS Microbiology Reviews* **25**:107–123. DOI: https://doi.org/10.1111/j.1574-6976.2001.tb00573.x, PMID: 11152942

Gao XD, Kaigorodov V, Jigami Y. 1999. YND1, a homologue of GDA1, encodes membrane-bound apyrase required for Golgi N- and O-glycosylation in *Saccharomyces cerevisiae*. *The Journal of Biological Chemistry* **274**:21450–21456. DOI: https://doi.org/10.1074/jbc.274.30.21450, PMID: 10409709

Gao J, Wang H, Li Z, Wong AH-H, Wang Y-Z, Guo Y, Lin X, Zeng G, Liu H, Wang Y, Wang J. 2018. Candida albicans gains azole resistance by altering sphingolipid composition. *Nature Communications* **9**:4495. DOI: https://doi.org/10.1038/s41467-018-06944-1, PMID: 30374049

García R, Botet J, Rodríguez-Peña JM, Bermejo C, Ribas JC, Revuelta JL, Nombela C, Arroyo J. 2015. Genomic profiling of fungal cell wall-interfering compounds: identification of a common gene signature. *BMC Genomics* **16**:683. DOI: https://doi.org/10.1186/s12864-015-1879-4, PMID: 26341223

Gasmi N, Jacques PE, Klimova N, Guo X, Ricciardi A, Robert F, Turcotte B. 2014. The switch from fermentation to respiration in *Saccharomyces cerevisiae* is regulated by the Ert1 transcriptional activator/repressor. *Genetics* **198**:547–560. DOI: https://doi.org/10.1534/genetics.114.168609, PMID: 25123508

Geva Y, Crissman J, Arakel EC, Gómez-Navarro N, Chuartzman SG, Stahmer KR, Schwappach B, Miller EA, Schuldiner M. 2017. Two novel effectors of trafficking and maturation of the yeast plasma membrane H^+-ATPase. *Traffic* **18**:672–682. DOI: https://doi.org/10.1111/tra.12503, PMID: 28727280

Giaever G, Shoemaker DD, Jones TW, Liang H, Winzeler EA, Astromoff A, Davis RW. 1999. Genomic profiling of drug sensitivities via induced haploinsufficiency. *Nature Genetics* **21**:278–283. DOI: https://doi.org/10.1038/6791, PMID: 10080179

Giaever G, Chu AM, Ni L, Connelly C, Riles L, Véronneau S, Dow S, Lucau-Danila A, Anderson K, André B, Arkin AP, Astromoff A, El-Bakkoury M, Bangham R, Benito R, Brachat S, Campanaro S, Curtiss M, Davis K, Deutschbauer A, et al. 2002. Functional profiling of the *Saccharomyces cerevisiae* genome. *Nature* **418**:387–391. DOI: https://doi.org/10.1038/nature00935, PMID: 12140549

Giaever G, Flaherty P, Kumm J, Proctor M, Nislow C, Jaramillo DF, Chu AM, Jordan MI, Arkin AP, Davis RW. 2004. Chemogenomic profiling: identifying the functional interactions of small molecules in yeast. *PNAS* **101**:793–798. DOI: https://doi.org/10.1073/pnas.0307490100, PMID: 14718668

Gietz RD, Schiestl RH. 2007. High-efficiency yeast transformation using the LiAc/SS carrier DNA/PEG method. *Nature Protocols* **2**:31–34. DOI: https://doi.org/10.1038/nprot.2007.13

Goossens A, de La Fuente N, Forment J, Serrano R, Portillo F. 2000. Regulation of yeast H(+)-ATPase by protein kinases belonging to a family dedicated to activation of plasma membrane transporters. *Molecular and Cellular Biology* **20**:7654–7661. DOI: https://doi.org/10.1128/MCB.20.20.7654-7661.2000, PMID: 11003661

Goy RC, de Britto D, Assis OBG. 2009. A review of the antimicrobial activity of chitosan. *Polímeros* **19**:241–247. DOI: https://doi.org/10.1590/S0104-14282009000300013

Gulshan K, Rovinsky SA, Coleman ST, Moye-Rowley WS. 2005. Oxidant-specific folding of Yap1p regulates both transcriptional activation and nuclear localization. *The Journal of Biological Chemistry* **280**:40524–40533. DOI: https://doi.org/10.1074/jbc.M504716200, PMID: 16219769

Gulshan K, Moye-Rowley WS. 2007. Multidrug resistance in fungi. *Eukaryotic Cell* **6**:1933–1942. DOI: https://doi.org/10.1128/EC.00254-07, PMID: 17873085

Guo Y, Park JM, Cui B, Humes E, Gangadharan S, Hung S, FitzGerald PC, Hoe KL, Grewal SIS, Craig NL, Levin HL. 2013. Integration profiling of gene function with dense maps of transposon integration. *Genetics* **195**:599–609. DOI: https://doi.org/10.1534/genetics.113.152744, PMID: 23893486

Hallstrom TC, Moye-Rowley WS. 2000. Multiple signals from dysfunctional mitochondria activate the pleiotropic drug resistance pathway in *Saccharomyces cerevisiae*. *Journal of Biological Chemistry* **275**:37347–37356. DOI: https://doi.org/10.1074/jbc.M007338200

Healey KR, Katiyar SK, Raj S, Edlind TD. 2012. CRS-MIS in *Candida glabrata*: sphingolipids modulate echinocandin-Fks interaction. *Molecular Microbiology* **86**:303–313. DOI: https://doi.org/10.1111/j.1365-2958.2012.08194.x, PMID: 22909030

Helander IM, Nurmiaho-Lassila EL, Ahvenainen R, Rhoades J, Roller S. 2001. Chitosan disrupts the barrier properties of the outer membrane of gram-negative bacteria. *International Journal of Food Microbiology* **71**:235–244. DOI: https://doi.org/10.1016/s0168-1605(01)00609-2, PMID: 11789941

Hillenmeyer ME, Fung E, Wildenhain J, Pierce SE, Hoon S, Lee W, Proctor M, St.Onge RP, Tyers M, Koller D, Altman RB, Davis RW, Nislow C, Giaever G. 2008. The chemical genomic portrait of yeast: uncovering a phenotype for all genes. *Science* **320**:362–365. DOI: https://doi.org/10.1126/science.1150021

Hoepfner D, Helliwell SB, Sadlish H, Schuierer S, Filipuzzi I, Brachat S, Bhullar B, Plikat U, Abraham Y, Altorfer M, Aust T, Baeriswyl L, Cerino R, Chang L, Estoppey D, Eichenberger J, Frederiksen M, Hartmann N, Hohendahl A,

Knapp B, et al. 2014. High-resolution chemical dissection of a model eukaryote reveals targets, pathways and gene functions. *Microbiological Research* **169**:107–120. DOI: https://doi.org/10.1016/j.micres.2013.11.004, PMID: 24360837

Hohmann S. 2002. Osmotic stress signaling and osmoadaptation in yeasts. *Microbiology and Molecular Biology Reviews* **66**:300–372. DOI: https://doi.org/10.1128/MMBR.66.2.300-372.2002

Hu Q, Luo Y. 2016. Polyphenol-chitosan conjugates: Synthesis, characterization, and applications. *Carbohydrate Polymers* **151**:624–639. DOI: https://doi.org/10.1016/j.carbpol.2016.05.109, PMID: 27474608

Jaime M, Lopez-Llorca LV, Conesa A, Lee AY, Proctor M, Heisler LE, Gebbia M, Giaever G, Westwood JT, Nislow C. 2012. Identification of yeast genes that confer resistance to chitosan oligosaccharide (COS) using chemogenomics. *BMC Genomics* **13**:267. DOI: https://doi.org/10.1186/1471-2164-13-267, PMID: 22727066

Janke C, Magiera MM, Rathfelder N, Taxis C, Reber S, Maekawa H, Moreno-Borchart A, Doenges G, Schwob E, Schiebel E, Knop M. 2004. A versatile toolbox for PCR-based tagging of yeast genes: new fluorescent proteins, more markers and promoter substitution cassettes. *Yeast* **21**:947–962. DOI: https://doi.org/10.1002/yea.1142, PMID: 15334558

Johansson P, Wiltschi B, Kumari P, Kessler B, Vonrhein C, Vonck J, Oesterhelt D, Grininger M. 2008. Inhibition of the fungal fatty acid synthase type I multienzyme complex. *PNAS* **105**:12803–12808. DOI: https://doi.org/10.1073/pnas.0805827105, PMID: 18725634

John Peter AT, van Schie SNS, Cheung NJ, Michel AH, Peter M, Kornmann B. 2022. Rewiring phospholipid biosynthesis reveals resilience to membrane perturbations and uncovers regulators of lipid homeostasis. *The EMBO Journal* **41**:e109998. DOI: https://doi.org/10.15252/embj.2021109998, PMID: 35188676

Jumper J, Evans R, Pritzel A, Green T, Figurnov M, Ronneberger O, Tunyasuvunakool K, Bates R, Žídek A, Potapenko A, Bridgland A, Meyer C, Kohl SAA, Ballard AJ, Cowie A, Romera-Paredes B, Nikolov S, Jain R, Adler J, Back T, et al. 2021. Highly accurate protein structure prediction with AlphaFold. *Nature* **596**:583–589. DOI: https://doi.org/10.1038/s41586-021-03819-2, PMID: 34265844

Jungwirth H, Wendler F, Platzer B, Bergler H, Högenauer G. 2000. Diazaborine resistance in yeast involves the efflux pumps Ycf1p and Flr1p and is enhanced by a gain-of-function allele of gene YAP1. *European Journal of Biochemistry* **267**:4809–4816. DOI: https://doi.org/10.1046/j.1432-1327.2000.01537.x, PMID: 10903515

Kaouass M, Audette M, Ramotar D, Verma S, De Montigny D, Gamache I, Torossian K, Poulin R. 1997. The STK2 gene, which encodes a putative Ser/Thr protein kinase, is required for high-affinity spermidine transport in *Saccharomyces cerevisiae*. *Molecular and Cellular Biology* **17**:2994–3004. DOI: https://doi.org/10.1128/MCB.17.6.2994, PMID: 9154797

Karadzas MT, Michel AH, Mosbach A, Giannakopoulos G, McGettigan R, Scalliet G, Kornmann B. 2026a. SATAY-based chemogenomic screening in *Saccharomyces cerevisiae*. *European Nucleotide Archive*. https://www.ebi.ac.uk/ena/browser/view/PRJEB129441

Karadzas MT, Michel AH, Mosbach A, Giannakopoulos G, McGettigan R, Scalliet G, Kornmann B. 2026b. *SATAY2.0. European Nucleotide Archive*. https://www.ebi.ac.uk/ena/browser/view/PRJEB35463

Karson EM, Ballou CE. 1978. Biosynthesis of yeast mannan. Properties of a mannosylphosphate transferase in *Saccharomyces cerevisiae*. *The Journal of Biological Chemistry* **253**:6484–6492. DOI: https://doi.org/10.1016/s0021-92581946958-5, PMID: 355255

Ke CL, Deng FS, Chuang CY, Lin CH. 2021. Antimicrobial actions and applications of chitosan. *Polymers* **13**:904. DOI: https://doi.org/10.3390/polym13060904, PMID: 33804268

Kehrein K, Schilling R, Möller-Hergt BV, Wurm CA, Jakobs S, Lamkemeyer T, Langer T, Ott M. 2015. Organization of mitochondrial gene expression in two distinct ribosome-containing assemblies. *Cell Reports* **10**:843–853. DOI: https://doi.org/10.1016/j.celrep.2015.01.012, PMID: 25683707

Kilani J, Fillinger S. 2016. Phenylpyrroles: 30 years, two molecules and (nearly) no resistance. *Frontiers in Microbiology* **7**:2014. DOI: https://doi.org/10.3389/fmicb.2016.02014, PMID: 28018333

Klopf E, Paskova L, Solé C, Mas G, Petryshyn A, Posas F, Wintersberger U, Ammerer G, Schüller C. 2009. Cooperation between the INO80 complex and histone chaperones determines adaptation of stress gene transcription in the yeast *Saccharomyces cerevisiae*. *Molecular and Cellular Biology* **29**:4994–5007. DOI: https://doi.org/10.1128/MCB.01858-08, PMID: 19620280

Ko CH, Buckley AM, Gaber RF. 1990. TRK2 is required for low affinity K+ transport in *Saccharomyces cerevisiae*. *Genetics* **125**:305–312. DOI: https://doi.org/10.1093/genetics/125.2.305, PMID: 2199312

Kojima K, Takano Y, Yoshimi A, Tanaka C, Kikuchi T, Okuno T. 2004. Fungicide activity through activation of a fungal signalling pathway. *Molecular Microbiology* **53**:1785–1796. DOI: https://doi.org/10.1111/j.1365-2958.2004.04244.x, PMID: 15341655

Kolaczkowski M, Kolaczowska A, Luczynski J, Witek S, Goffeau A. 1998. In vivo characterization of the drug resistance profile of the major ABC transporters and other components of the yeast pleiotropic drug resistance network. *Microbial Drug Resistance* **4**:143–158. DOI: https://doi.org/10.1089/mdr.1998.4.143, PMID: 9818966

Kong M, Chen XG, Xing K, Park HJ. 2010. Antimicrobial properties of chitosan and mode of action: a state of the art review. *International Journal of Food Microbiology* **144**:51–63. DOI: https://doi.org/10.1016/j.ijfoodmicro.2010.09.012, PMID: 20951455

Kuge S, Jones N, Nomoto A. 1997. Regulation of yAP-1 nuclear localization in response to oxidative stress. *The EMBO Journal* **16**:1710–1720. DOI: https://doi.org/10.1093/emboj/16.7.1710, PMID: 9130715

Kuhn NJ, Ward S, Leong WS. 1991. Submicromolar manganese dependence of Golgi vesicular galactosyltransferase (lactose synthetase). *European Journal of Biochemistry* **195**:243–250. DOI: https://doi.org/10.1111/j.1432-1033.1991.tb15700.x, PMID: 1899383

Lanthaler K, Bilsland E, Dobson PD, Moss HJ, Pir P, Kell DB, Oliver SG. 2011. Genome-wide assessment of the carriers involved in the cellular uptake of drugs: a model system in yeast. *BMC Biology* **9**:70. DOI: https://doi.org/10.1186/1741-7007-9-70, PMID: 22023736

Lawry SM, Tebbets B, Kean I, Stewart D, Hetelle J, Klein BS. 2017. Fludioxonil induces Drk1, a fungal group III hybrid histidine kinase, to dephosphorylate its downstream target, Ypd1. *Antimicrobial Agents and Chemotherapy* **61**:e01414-16. DOI: https://doi.org/10.1128/AAC.01414-16

Lee AY, St.Onge RP, Proctor MJ, Wallace IM, Nile AH, Spagnuolo PA, Jitkova Y, Gronda M, Wu Y, Kim MK, Cheung-Ong K, Torres NP, Spear ED, Han MKL, Schlecht U, Suresh S, Duby G, Heisler LE, Surendra A, Fung E, et al. 2014. Mapping the cellular response to small molecules using chemogenomic fitness signatures. *Science* **344**:208–211. DOI: https://doi.org/10.1126/science.1250217

Leroux P, Lanen C, Fritz R. 1992. Similarities in the antifungal activities of fenpiclonil, iprodione and tolclofos-methyl against *Botrytis cinerea* and *Fusarium nivale*. *Pesticide Science* **36**:255–261. DOI: https://doi.org/10.1002/ps.2780360312

Lesage G, Sdicu AM, Ménard P, Shapiro J, Hussein S, Bussey H. 2004. Analysis of beta-1,3-glucan assembly in *Saccharomyces cerevisiae* using a synthetic interaction network and altered sensitivity to caspofungin. *Genetics* **167**:35–49. DOI: https://doi.org/10.1534/genetics.167.1.35, PMID: 15166135

Levitan A, Gale AN, Dallon EK, Kozan DW, Cunningham KW, Sharan R, Berman J. 2020. Comparing the utility of in vivo transposon mutagenesis approaches in yeast species to infer gene essentiality. *Current Genetics* **66**:1117–1134. DOI: https://doi.org/10.1007/s00294-020-01096-6

Li J, Zhang JM, Li X, Suo F, Zhang MJ, Hou W, Han J, Du LL. 2011. A piggyBac transposon-based mutagenesis system for the fission yeast *Schizosaccharomyces pombe*. *Nucleic Acids Research* **39**:e40. DOI: https://doi.org/10.1093/nar/gkq1358

Li R, Zhu L, Liu D, Wang W, Zhang C, Jiao S, Wei J, Ren L, Zhang Y, Gou X, Yuan X, Du Y, Wang ZA. 2022. High molecular weight chitosan oligosaccharide exhibited antifungal activity by misleading cell wall organization via targeting PHR transglucosidases. *Carbohydrate Polymers* **285**:119253. DOI: https://doi.org/10.1016/j.carbpol.2022.119253, PMID: 35287867

Li L, Short FL, Hassan KA, Naidu V, Pokhrel A, Nagy SS, Prity FT, Shah BS, Afrin N, Baker S, Parkhill J, Cain AK, Paulsen IT. 2023. Systematic analyses identify modes of action of ten clinically relevant biocides and antibiotic antagonism in *Acinetobacter baumannii*. *Nature Microbiology* **8**:1995–2005. DOI: https://doi.org/10.1038/s41564-023-01474-z

Liu H, Du Y, Wang X, Sun L. 2004. Chitosan kills bacteria through cell membrane damage. *International Journal of Food Microbiology* **95**:147–155. DOI: https://doi.org/10.1016/j.ijfoodmicro.2004.01.022, PMID: 15282127

Longtine MS, McKenzie A, Demarini DJ, Shah NG, Wach A, Brachat A, Philippsen P, Pringle JR. 1998. Additional modules for versatile and economical PCR-based gene deletion and modification in *Saccharomyces cerevisiae*. *Yeast* **14**:953–961. DOI: https://doi.org/10.1002/(SICI)1097-0061(199807)14:10<953::AID-YEA293>3.0.CO;2-U, PMID: 9717241

Luk EEC, Culotta VC. 2001. Manganese superoxide dismutase in *Saccharomyces cerevisiae* acquires its metal co-factor through a pathway involving the Nramp metal transporter, Smf2p. *Journal of Biological Chemistry* **276**:47556–47562. DOI: https://doi.org/10.1074/jbc.M108923200

Ma Z, Garrido-Maestu A, Jeong KC. 2017. Application, mode of action, and in vivo activity of chitosan and its micro- and nanoparticles as antimicrobial agents: a review. *Carbohydrate Polymers* **176**:257–265. DOI: https://doi.org/10.1016/j.carbpol.2017.08.082

Madrid R, Gómez MJ, Ramos J, Rodríguez-Navarro A. 1998. Ectopic potassium uptake in trk1 trk2 mutants of *Saccharomyces cerevisiae* correlates with a highly hyperpolarized membrane potential. *The Journal of Biological Chemistry* **273**:14838–14844. DOI: https://doi.org/10.1074/jbc.273.24.14838, PMID: 9614085

Maeda T, Wurgler-Murphy SM, Saito H. 1994. A two-component system that regulates an osmosensing MAP kinase cascade in yeast. *Nature* **369**:242–245. DOI: https://doi.org/10.1038/369242a0, PMID: 8183345

Marcireau C, Guilloton M, Karst F. 1990. In vivo effects of fenpropimorph on the yeast *Saccharomyces cerevisiae* and determination of the molecular basis of the antifungal property. *Antimicrobial Agents and Chemotherapy* **34**:989–993. DOI: https://doi.org/10.1128/AAC.34.6.989

Markovich S, Yekutiel A, Shalit I, Shadkchan Y, Osherov N. 2004. Genomic approach to identification of mutations affecting caspofungin susceptibility in *Saccharomyces cerevisiae*. *Antimicrobial Agents and Chemotherapy* **48**:3871–3876. DOI: https://doi.org/10.1128/AAC.48.10.3871-3876.2004

Martel CM, Parker JE, Bader O, Weig M, Gross U, Warrilow AGS, Kelly DE, Kelly SL. 2010. A clinical isolate of *Candida albicans* with mutations in *ERG11* (Encoding Sterol 14α-Demethylase) and *ERG5* (Encoding C22 Desaturase) is cross resistant to Azoles and Amphotericin B . *Antimicrobial Agents and Chemotherapy* **54**:3578–3583. DOI: https://doi.org/10.1128/AAC.00303-10

Mas G, de Nadal E, Dechant R, de la Concepción MLR, Logie C, Jimeno-González S, Chávez S, Ammerer G, Posas F. 2009. Recruitment of a chromatin remodelling complex by the Hog1 MAP kinase to stress genes. *The EMBO Journal* **28**:326–336. DOI: https://doi.org/10.1038/emboj.2008.299

Meena N, Kaur H, Mondal AK. 2010. Interactions among HAMP domain repeats act as an osmosensing molecular switch in group III hybrid histidine kinases from fungi. *The Journal of Biological Chemistry* **285**:12121–12132. DOI: https://doi.org/10.1074/jbc.M109.075721, PMID: 20164185

Mellegård H, Strand SP, Christensen BE, Granum PE, Hardy SP. 2011. Antibacterial activity of chemically defined chitosans: Influence of molecular weight, degree of acetylation and test organism. *International Journal of Food Microbiology* **148**:48–54. DOI: https://doi.org/10.1016/j.ijfoodmicro.2011.04.023

Meyers S, Schauer W, Balzi E, Wagner M, Goffeau A, Golin J. 1992. Interaction of the yeast pleiotropic drug resistance genes PDR1 and PDR5. *Current Genetics* **21**:431–436. DOI: https://doi.org/10.1007/BF00351651, PMID: 1319843

Michel AH, Hatakeyama R, Kimmig P, Arter M, Peter M, Matos J, De Virgilio C, Kornmann B. 2017. Functional mapping of yeast genomes by saturated transposition. *eLife* **6**:e23570. DOI: https://doi.org/10.7554/eLife.23570, PMID: 28481201

Michel AH, Kornmann B. 2022. SAturated transposon analysis in yeast (SATAY) for deep functional mapping of yeast genomes. In: Devaux F (Ed). *Yeast Functional Genomics*. Springer US. p. 349–379. DOI: https://doi.org/10.1007/978-1-0716-2257-5_20

Mielich K, Shtifman-Segal E, Golz JC, Zeng G, Wang Y, Berman J, Kunze R. 2018. Maize transposable elements Ac/Ds as insertion mutagenesis tools in Candida albicans. *G3: Genes, Genomes, Genetics* **8**:1139–1145. DOI: https://doi.org/10.1534/g3.117.300388, PMID: 29378819

Mitsuyama J, Nomura N, Hashimoto K, Yamada E, Nishikawa H, Kaeriyama M, Kimura A, Todo Y, Narita H. 2008. In vitro and in vivo antifungal activities of T-2307, a novel arylamidine. *Antimicrobial Agents and Chemotherapy* **52**:1318–1324. DOI: https://doi.org/10.1128/AAC.01159-07

Miyake Y, Kozutsumi Y, Nakamura S, Fujita T, Kawasaki T. 1995. Serine palmitoyltransferase is the primary target of a sphingosine-like immunosuppressant, ISP-1/myriocin. *Biochemical and Biophysical Research Communications* **211**:396–403. DOI: https://doi.org/10.1006/bbrc.1995.1827, PMID: 7794249

Mortimer RK, Johnston JR. 1986. Genealogy of principal strains of the yeast genetic stock center. *Genetics* **113**:35–43. DOI: https://doi.org/10.1093/genetics/113.1.35, PMID: 3519363

Motoyama T, Ohira T, Kadokura K, Ichiishi A, Fujimura M, Yamaguchi I, Kudo T. 2005. An Os-1 family histidine kinase from a filamentous fungus confers fungicide-sensitivity to yeast. *Current Genetics* **47**:298–306. DOI: https://doi.org/10.1007/s00294-005-0572-6, PMID: 15776234

Moye-Rowley WS. 2003. Transcriptional control of multidrug resistance in the yeast *Saccharomyces*. *Progress in Nucleic Acid Research and Molecular Biology* **73**:251–279. DOI: https://doi.org/10.1016/s0079-6603(03)01008-0, PMID: 12882520

Mulet JM, Leube MP, Kron SJ, Rios G, Fink GR, Serrano R. 1999. A novel mechanism of ion homeostasis and salt tolerance in yeast: the Hal4 and Hal5 protein kinases modulate the Trk1-Trk2 potassium transporter. *Molecular and Cellular Biology* **19**:3328–3337. DOI: https://doi.org/10.1128/MCB.19.5.3328, PMID: 10207057

Munro S. 2001. What can yeast tell us about N-linked glycosylation in the Golgi apparatus? *FEBS Letters* **498**:223–227. DOI: https://doi.org/10.1016/s0014-5793(01)02488-7, PMID: 11412862

Murray JL, Kwon T, Marcotte EM, Whiteley M. 2015. Intrinsic antimicrobial resistance determinants in the superbug *Pseudomonas aeruginosa*. *mBio* **6**:e01603-15. DOI: https://doi.org/10.1128/mBio.01603-15, PMID: 26507235

Myer VE, Young RA. 1998. RNA polymerase II holoenzymes and subcomplexes. *The Journal of Biological Chemistry* **273**:27757–27760. DOI: https://doi.org/10.1074/jbc.273.43.27757, PMID: 9774381

Nadal-Ribelles M, Conde N, Flores O, González-Vallinas J, Eyras E, Orozco M, de Nadal E, Posas F. 2012. Hog1 bypasses stress-mediated down-regulation of transcription by RNA polymerase II redistribution and chromatin remodeling. *Genome Biology* **13**:R106. DOI: https://doi.org/10.1186/gb-2012-13-11-r106, PMID: 23158682

Nakajima T, Ballou CE. 1975. Yeast manno-protein biosynthesis: solubilization and selective assay of four mannosyltransferases. *PNAS* **72**:3912–3916. DOI: https://doi.org/10.1073/pnas.72.10.3912, PMID: 1105568

Nemecek JC, Wüthrich M, Klein BS. 2006. Global control of dimorphism and virulence in fungi. *Science* **312**:583–588. DOI: https://doi.org/10.1126/science.1124105, PMID: 16645097

Nickels TJ, Gale AP, Harrington AA, Timp W, Cunningham KW. 2024. Tn-Seq of the *Candida glabrata* reference strain CBS138 reveals epigenetic plasticity, structural variation, and intrinsic mechanisms of resistance to micafungin. *bioRxiv*. DOI: https://doi.org/10.1101/2024.05.02.592251

Nishikawa H, Yamada E, Shibata T, Uchihashi S, Fan H, Hayakawa H, Nomura N, Mitsuyama J. 2010. Uptake of T-2307, a novel arylamidine, in *Candida albicans*. *The Journal of Antimicrobial Chemotherapy* **65**:1681–1687. DOI: https://doi.org/10.1093/jac/dkq177, PMID: 20513704

Nishikawa H, Sakagami T, Yamada E, Fukuda Y, Hayakawa H, Nomura N, Mitsuyama J, Miyazaki T, Mukae H, Kohno S. 2016. T-2307, a novel arylamidine, is transported into *Candida albicans* by a high-affinity spermine and spermidine carrier regulated by Agp2. *The Journal of Antimicrobial Chemotherapy* **71**:1845–1855. DOI: https://doi.org/10.1093/jac/dkw095, PMID: 27090633

Nishikawa H, Fukuda Y, Mitsuyama J, Tashiro M, Tanaka A, Takazono T, Saijo T, Yamamoto K, Nakamura S, Imamura Y, Miyazaki T, Kakeya H, Yamamoto Y, Yanagihara K, Mukae H, Kohno S, Izumikawa K. 2017. In vitro and in vivo antifungal activities of T-2307, a novel arylamidine, against Cryptococcus gattii: an emerging fungal pathogen. *The Journal of Antimicrobial Chemotherapy* **72**:1709–1713. DOI: https://doi.org/10.1093/jac/dkx020, PMID: 28201509

Odani T, Shimma YI, Tanaka A, Jigami Y. 1996. Cloning and analysis of the MNN4 gene required for phosphorylation of N-linked oligosaccharides in *Saccharomyces cerevisiae*. *Glycobiology* **6**:805–810. DOI: https://doi.org/10.1093/glycob/6.8.805, PMID: 9023541

Orlean P. 2012. Architecture and biosynthesis of the *Saccharomyces cerevisiae* cell wall. *Genetics* **192**:775–818. DOI: https://doi.org/10.1534/genetics.112.144485, PMID: 23135325

Oskouian B, Saba JD. 1999. YAP1 confers resistance to the fatty acid synthase inhibitor cerulenin through the transporter Flr1p in *Saccharomyces cerevisiae*. *Molecular and General Genetics MGG* **261**:346–353. DOI: https://doi.org/10.1007/s004380050975

Ota IM, Varshavsky A. 1993. A yeast protein similar to bacterial two-component regulators. *Science* **262**:566–569. DOI: https://doi.org/10.1126/science.8211183
Palma-Guerrero J, Lopez-Jimenez JA, Pérez-Berná AJ, Huang IC, Jansson HB, Salinas J, Villalaín J, Read ND, Lopez-Llorca LV. 2010. Membrane fluidity determines sensitivity of filamentous fungi to chitosan. *Molecular Microbiology* **75**:1021–1032. DOI: https://doi.org/10.1111/j.1365-2958.2009.07039.x, PMID: 20487294
Palmeira-de-Oliveira A, Passarinha LA, Gaspar C, Palmeira-de-Oliveira R, Sarmento B, Martinez-de-Oliveira J, Pina-Vaz C, Rodrigues AG, Queiroz JA. 2011. The relationship between Candida species charge density and chitosan activity evaluated by ion-exchange chromatography. *Journal of Chromatography B* **879**:3749–3751. DOI: https://doi.org/10.1016/j.jchromb.2011.07.034
Parsons AB, Brost RL, Ding H, Li Z, Zhang C, Sheikh B, Brown GW, Kane PM, Hughes TR, Boone C. 2004. Integration of chemical-genetic and genetic interaction data links bioactive compounds to cellular target pathways. *Nature Biotechnology* **22**:62–69. DOI: https://doi.org/10.1038/nbt919, PMID: 14661025
Patterson K, Yu J, Landberg J, Chang I, Shavarebi F, Bilanchone V, Sandmeyer S. 2018. Functional genomics for the oleaginous yeast Yarrowia lipolytica. *Metabolic Engineering* **48**:184–196. DOI: https://doi.org/10.1016/j.ymben.2018.05.008, PMID: 29792930
Pavesic MW, Gale AN, Nickels TJ, Harrington AA, Bussey M, Cunningham KW. 2024. Calcineurin-dependent contributions to fitness in the opportunistic pathogen *Candida glabrata mSphere* **9**:e0055423. DOI: https://doi.org/10.1128/msphere.00554-23, PMID: 38171022
Pérez-Valle J, Jenkins H, Merchan S, Montiel V, Ramos J, Sharma S, Serrano R, Yenush L. 2007. Key role for intracellular K^+ and protein kinases Sat4/Hal4 and Hal5 in the plasma membrane stabilization of yeast nutrient transporters . *Molecular and Cellular Biology* **27**:5725–5736. DOI: https://doi.org/10.1128/MCB.01375-06
Perfect JR. 2017. The antifungal pipeline: a reality check. *Nature Reviews Drug Discovery* **16**:603–616. DOI: https://doi.org/10.1038/nrd.2017.46
Perlin DS, Rautemaa-Richardson R, Alastruey-Izquierdo A. 2017. The global problem of antifungal resistance: prevalence, mechanisms, and management. *The Lancet Infectious Diseases* **17**:e383–e392. DOI: https://doi.org/10.1016/S1473-3099(17)30316-X
Pokrovskaya ID, Willett R, Smith RD, Morelle W, Kudlyk T, Lupashin VV. 2011. Conserved oligomeric Golgi complex specifically regulates the maintenance of Golgi glycosylation machinery. *Glycobiology* **21**:1554–1569. DOI: https://doi.org/10.1093/glycob/cwr028, PMID: 21421995
Posas F, Wurgler-Murphy SM, Maeda T, Witten EA, Thai TC, Saito H. 1996. Yeast HOG1 MAP kinase cascade is regulated by a multistep phosphorelay mechanism in the SLN1–YPD1–SSK1 "Two-Component" osmosensor. *Cell* **86**:865–875. DOI: https://doi.org/10.1016/S0092-8674(00)80162-2
Prasad R, Goffeau A. 2012. Yeast ATP-binding cassette transporters conferring multidrug resistance. *Annual Review of Microbiology* **66**:39–63. DOI: https://doi.org/10.1146/annurev-micro-092611-150111, PMID: 22703054
Proft M, Struhl K. 2002. Hog1 kinase converts the Sko1-Cyc8-Tup1 repressor complex into an activator that recruits SAGA and SWI/SNF in response to osmotic stress. *Molecular Cell* **9**:1307–1317. DOI: https://doi.org/10.1016/s1097-2765(02)00557-9, PMID: 12086627
Puumala E, Fallah S, Robbins N, Cowen LE. 2024. Advancements and challenges in antifungal therapeutic development. *Clinical Microbiology Reviews* **37**:e0014223. DOI: https://doi.org/10.1128/cmr.00142-23, PMID: 38294218
Qin Y, Li P. 2020. Antimicrobial chitosan conjugates: current synthetic strategies and potential applications. *International Journal of Molecular Sciences* **21**:499. DOI: https://doi.org/10.3390/ijms21020499, PMID: 31941068
Raafat D, von Bargen K, Haas A, Sahl H-G. 2008. Insights into the mode of action of chitosan as an antibacterial compound. *Applied and Environmental Microbiology* **74**:3764–3773. DOI: https://doi.org/10.1128/AEM.00453-08, PMID: 18456858
Randhawa A, Kundu D, Sharma A, Prasad R, Mondal AK. 2019. Overexpression of the CORVET complex alleviates the fungicidal effects of fludioxonil on the yeast *Saccharomyces cerevisiae* expressing hybrid histidine kinase 3. *The Journal of Biological Chemistry* **294**:461–475. DOI: https://doi.org/10.1074/jbc.RA118.004736, PMID: 30446623
Raschke WC, Kern KA, Antalis C, Ballou CE. 1973. Genetic control of yeast Mannan structure. *Journal of Biological Chemistry* **248**:4660–4666. DOI: https://doi.org/10.1016/S0021-9258(19)43714-9
Regelmann J, Schüle T, Josupeit FS, Horak J, Rose M, Entian K-D, Thumm M, Wolf DH. 2003. Catabolite degradation of fructose-1,6-bisphosphatase in the yeast *Saccharomyces cerevisiae*: a genome-wide screen identifies eight novel GID genes and indicates the existence of two degradation pathways. *Molecular Biology of the Cell* **14**:1652–1663. DOI: https://doi.org/10.1091/mbc.e02-08-0456, PMID: 12686616
Robbins N, Caplan T, Cowen LE. 2017. Molecular evolution of antifungal drug resistance. *Annual Review of Microbiology* **71**:753–775. DOI: https://doi.org/10.1146/annurev-micro-030117-020345, PMID: 28886681
Robbins N, Cowen LE. 2022. Antifungal discovery. *Current Opinion in Microbiology* **69**:102198. DOI: https://doi.org/10.1016/j.mib.2022.102198, PMID: 36037637
Rogers B, Decottignies A, Kolaczkowski M, Carvajal E, Balzi E, Goffeau A. 2001. The pleitropic drug ABC transporters from *Saccharomyces cerevisiae*. *Journal of Molecular Microbiology and Biotechnology* **3**:207–214 PMID: 11321575.
Ryu H, Park H, Suh DS, Jung GH, Park K, Lee BD. 2014. Biological control of Colletotrichum panacicola on Panax ginseng by *Bacillus subtilis* HK-CSM-1. *Journal of Ginseng Research* **38**:215–219. DOI: https://doi.org/10.1016/j.jgr.2014.05.001, PMID: 25378997

Sá-Correia I, dos Santos SC, Teixeira MC, Cabrito TR, Mira NP. 2009. Drug:H+ antiporters in chemical stress response in yeast. *Trends in Microbiology* **17**:22–31. DOI: https://doi.org/10.1016/j.tim.2008.09.007, PMID: 19062291

Sanchez MR, Payen C, Cheong F, Hovde BT, Bissonnette S, Arkin AP, Skerker JM, Brem RB, Caudy AA, Dunham MJ. 2019. Transposon insertional mutagenesis in *Saccharomyces uvarum* reveals *trans*-acting effects influencing species-dependent essential genes. *Genome Research* **29**:396–406. DOI: https://doi.org/10.1101/gr.232330.117, PMID: 30635343

Sardana R, Highland CM, Straight BE, Chavez CF, Fromme JC, Emr SD. 2021. Golgi membrane protein Erd1 Is essential for recycling a subset of Golgi glycosyltransferases. *eLife* **10**:e70774. DOI: https://doi.org/10.7554/eLife.70774, PMID: 34821548

Satish S, Perlin DS. 2019. Echinocandin resistance in *Aspergillus fumigatus* has broad implications for membrane lipid perturbations that influence drug-target interactions. *Microbiology Insights* **12**:1178636119897034. DOI: https://doi.org/10.1177/1178636119897034, PMID: 35185336

Schüle T, Rose M, Entian KD, Thumm M, Wolf DH. 2000. Ubc8p functions in catabolite degradation of fructose-1, 6-bisphosphatase in yeast. *The EMBO Journal* **19**:2161–2167. DOI: https://doi.org/10.1093/emboj/19.10.2161, PMID: 10811607

Segal ES, Gritsenko V, Levitan A, Yadav B, Dror N, Steenwyk JL, Silberberg Y, Mielich K, Rokas A, Gow NAR, Kunze R, Sharan R, Berman J. 2018. Gene essentiality analyzed by in vivo transposon mutagenesis and machine learning in a stable haploid isolate of *Candida albicans*. *mBio* **9**:e02048-18. DOI: https://doi.org/10.1128/mBio.02048-18

Serbyn N, Noireterre A, Bagdiul I, Plank M, Michel AH, Loewith R, Kornmann B, Stutz F. 2020. The aspartic protease Ddi1 contributes to DNA-protein crosslink repair in yeast. *Molecular Cell* **77**:1066–1079. DOI: https://doi.org/10.1016/j.molcel.2019.12.007, PMID: 31902667

Serrano R, Kielland-Brandt MC, Fink GR. 1986. Yeast plasma membrane ATPase is essential for growth and has homology with (Na+ + K+), K+- and Ca2+-ATPases. *Nature* **319**:689–693. DOI: https://doi.org/10.1038/319689a0, PMID: 3005867

Servos J, Haase E, Brendel M. 1993. Gene SNQ2 of *Saccharomyces cerevislae*, which confers resistance to 4-nitroquinoline-N-oxide and other chemicals, encodes a 169 kDa protein homologous to ATP-dependent permeases. *Molecular and General Genetics MGG* **236**:214–218. DOI: https://doi.org/10.1007/BF00277115

Setty SRG, Shin ME, Yoshino A, Marks MS, Burd CG. 2003. Golgi recruitment of GRIP domain proteins by Arf-like GTPase 1 is regulated by Arf-like GTPase 3. *Current Biology* **13**:401–404. DOI: https://doi.org/10.1016/S0960-9822(03)00089-7

Shestakova A, Zolov S, Lupashin V. 2006. COG complex-mediated recycling of Golgi glycosyltransferases is essential for normal protein glycosylation. *Traffic* **7**:191–204. DOI: https://doi.org/10.1111/j.1600-0854.2005.00376.x, PMID: 16420527

Shibata T, Takahashi T, Yamada E, Kimura A, Nishikawa H, Hayakawa H, Nomura N, Mitsuyama J. 2012. T-2307 causes collapse of mitochondrial membrane potential in yeast. *Antimicrobial Agents and Chemotherapy* **56**:5892–5897. DOI: https://doi.org/10.1128/AAC.05954-11

Shih PY, Liao YT, Tseng YK, Deng FS, Lin CH. 2019. A potential antifungal effect of chitosan against *Candida albicans* is mediated via the inhibition of SAGA complex component expression and the subsequent alteration of cell surface integrity. *Frontiers in Microbiology* **10**:602. DOI: https://doi.org/10.3389/fmicb.2019.00602, PMID: 30972050

Sikorski RS, Hieter P. 1989. A system of shuttle vectors and yeast host strains designed for efficient manipulation of DNA in *Saccharomyces cerevisiae*. *Genetics* **122**:19–27. DOI: https://doi.org/10.1093/genetics/122.1.19, PMID: 2659436

Soontorngun N, Larochelle M, Drouin S, Robert F, Turcotte B. 2007. Regulation of gluconeogenesis in *Saccharomyces cerevisiae* is mediated by activator and repressor functions of Rds2. *Molecular and Cellular Biology* **27**:7895–7905. DOI: https://doi.org/10.1128/MCB.01055-07, PMID: 17875938

Steinberg G, Gurr SJ. 2020. Fungi, fungicide discovery and global food security. *Fungal Genetics and Biology* **144**:103476. DOI: https://doi.org/10.1016/j.fgb.2020.103476

Stratford M. 1992. Yeast flocculation: reconciliation of physiological and genetic viewpoints. *Yeast* **8**:25–38. DOI: https://doi.org/10.1002/yea.320080103

Suzuki Y, St Onge RP, Mani R, King OD, Heilbut A, Labunskyy VM, Chen W, Pham L, Zhang LV, Tong AHY, Nislow C, Giaever G, Gladyshev VN, Vidal M, Schow P, Lehár J, Roth FP. 2011. Knocking out multigene redundancies via cycles of sexual assortment and fluorescence selection. *Nature Methods* **8**:159–164. DOI: https://doi.org/10.1038/nmeth.1550, PMID: 21217751

Tayel AA, Moussa S, El-Tras WF, Knittel D, Opwis K, Schollmeyer E. 2010. Anticandidal action of fungal chitosan against *Candida albicans*. *International Journal of Biological Macromolecules* **47**:454–457. DOI: https://doi.org/10.1016/j.ijbiomac.2010.06.011

Teng X, Dayhoff-Brannigan M, Cheng WC, Gilbert CE, Sing CN, Diny NL, Wheelan SJ, Dunham MJ, Boeke JD, Pineda FJ, Hardwick JM. 2013. Genome-wide consequences of deleting any single gene. *Molecular Cell* **52**:485–494. DOI: https://doi.org/10.1016/j.molcel.2013.09.026, PMID: 24211263

Tillman RW, Siegel MR, Long JW. 1973. Mechanism of action and fate of the fungicide chlorothalonil (2,4,5,6-tetrachloroisophthalonitrile) in biological systems. *Pesticide Biochemistry and Physiology* **3**:160–167. DOI: https://doi.org/10.1016/0048-3575(73)90100-4

Tkacz JS, Lampen JO. 1975. Tunicamycin inhibition of polyisoprenyl N-acetylglucosaminyl pyrophosphate formation in calf-liver microsomes. *Biochemical and Biophysical Research Communications* **65**:248–257. DOI: https://doi.org/10.1016/S0006-291X(75)80086-6

Tsai GJ, Su WH. 1999. Antibacterial activity of Shrimp Chitosan against *Escherichia coli*. *Journal of Food Protection* **62**:239–243. DOI: https://doi.org/10.4315/0362-028X-62.3.239

van Opijnen T, Bodi KL, Camilli A. 2009. Tn-seq: high-throughput parallel sequencing for fitness and genetic interaction studies in microorganisms. *Nature Methods* **6**:767–772. DOI: https://doi.org/10.1038/nmeth.1377

Verlee A, Mincke S, Stevens CV. 2017. Recent developments in antibacterial and antifungal chitosan and its derivatives. *Carbohydrate Polymers* **164**:268–283. DOI: https://doi.org/10.1016/j.carbpol.2017.02.001

Vindu A, Shin BS, Choi K, Christenson ET, Ivanov IP, Cao C, Banerjee A, Dever TE. 2021. Translational autoregulation of the *S. cerevisiae* high-affinity polyamine transporter Hol1. *Molecular Cell* **81**:3904–3918. DOI: https://doi.org/10.1016/j.molcel.2021.07.020, PMID: 34375581

Wang X-H, Nakayama K, Shimma Y, Tanaka A, Jigami Y. 1997. MNN6, a Member of the KRE2/MNT1 family, is the gene for mannosylphosphate transfer in *Saccharomyces cerevisiae*. *Journal of Biological Chemistry* **272**:18117–18124. DOI: https://doi.org/10.1074/jbc.272.29.18117

Whitney PA, Morris DR. 1978. Polyamine auxotrophs of *Saccharomyces cerevisiae*. *Journal of Bacteriology* **134**:214–220. DOI: https://doi.org/10.1128/jb.134.1.214-220.1978

Wiederhold NP, Najvar LK, Fothergill AW, Bocanegra R, Olivo M, McCarthy DI, Kirkpatrick WR, Fukuda Y, Mitsuyama J, Patterson TF. 2015. The novel Arylamidine T-2307 maintains *in vitro* and *in vivo* activity against echinocandin-resistant *Candida albicans*. *Antimicrobial Agents and Chemotherapy* **59**:1341–1343. DOI: https://doi.org/10.1128/AAC.04228-14

Wiederhold NP, Najvar LK, Fothergill AW, Bocanegra R, Olivo M, McCarthy DI, Fukuda Y, Mitsuyama J, Patterson TF. 2016. The novel arylamidine T-2307 demonstrates in vitro and in vivo activity against echinocandin-resistant *Candida glabrata*. *The Journal of Antimicrobial Chemotherapy* **71**:692–695. DOI: https://doi.org/10.1093/jac/dkv398, PMID: 26620102

Wiederhold NP, Najvar LK, Jaramillo R, Olivo M, Patterson H, Connell A, Fukuda Y, Mitsuyama J, Catano G, Patterson TF. 2020. The novel Arylamidine T-2307 demonstrates in vitro and in vivo activity against *Candida auris*. *Antimicrobial Agents and Chemotherapy* **64**:5–9. DOI: https://doi.org/10.1128/AAC.02198-19

Wiederhold NP. 2021. Review of T-2307, an investigational agent that causes collapse of fungal mitochondrial membrane potential. *Journal of Fungi* **7**:1–9. DOI: https://doi.org/10.3390/jof7020130, PMID: 33670132

Winzeler EA, Shoemaker DD, Astromoff A, Liang H, Anderson K, Andre B, Bangham R, Benito R, Boeke JD, Bussey H, Chu AM, Connelly C, Davis K, Dietrich F, Dow SW, El Bakkoury M, Foury F, Friend SH, Gentalen E, Giaever G, et al. 1999. Functional characterization of the *S. cerevisiae* genome by gene deletion and parallel analysis. *Science* **285**:901–906. DOI: https://doi.org/10.1126/science.285.5429.901, PMID: 10436161

Wright MB, Howell EA, Gaber RF. 1996. Amino acid substitutions in membrane-spanning domains of Hol1, a member of the major facilitator superfamily of transporters, confer nonselective cation uptake in *Saccharomyces cerevisiae*. *Journal of Bacteriology* **178**:7197–7205. DOI: https://doi.org/10.1128/jb.178.24.7197-7205.1996, PMID: 8955402

Xu Z, Wei W, Gagneur J, Perocchi F, Clauder-Münster S, Camblong J, Guffanti E, Stutz F, Huber W, Steinmetz LM. 2009. Bidirectional promoters generate pervasive transcription in yeast. *Nature* **457**:1033–1037. DOI: https://doi.org/10.1038/nature07728

Yamashita K, Miyazaki T, Fukuda Y, Mitsuyama J, Saijo T, Shimamura S, Yamamoto K, Imamura Y, Izumikawa K, Yanagihara K, Kohno S, Mukae H. 2019. The novel Arylamidine T-2307 selectively disrupts yeast mitochondrial function by inhibiting respiratory chain complexes. *Antimicrobial Agents and Chemotherapy* **63**:e00374-19. DOI: https://doi.org/10.1128/AAC.00374-19

Yip CL, Welch SK, Klebl F, Gilbert T, Seidel P, Grant FJ, O'Hara PJ, MacKay VL. 1994. Cloning and analysis of the *Saccharomyces cerevisiae* MNN9 and MNN1 genes required for complex glycosylation of secreted proteins. *PNAS* **91**:2723–2727. DOI: https://doi.org/10.1073/pnas.91.7.2723, PMID: 8146181

Yu J, Marshall K, Yamaguchi M, Haber JE, Weil CF. 2004. Microhomology-dependent end joining and repair of transposon-induced DNA hairpins by host factors in *Saccharomyces cerevisiae* . *Molecular and Cellular Biology* **24**:1351–1364. DOI: https://doi.org/10.1128/MCB.24.3.1351-1364.2004

Yu CJ, Lee FJS. 2017. Multiple activities of Arl1 GTPase in the trans-Golgi network. *Journal of Cell Science* **130**:1691–1699. DOI: https://doi.org/10.1242/jcs.201319

Zakrzewska A, Boorsma A, Brul S, Hellingwerf KJ, Klis FM. 2005. Transcriptional response of *Saccharomyces cerevisiae* to the plasma membrane-perturbing compound chitosan. *Eukaryotic Cell* **4**:703–715. DOI: https://doi.org/10.1128/EC.4.4.703-715.2005, PMID: 15821130

Zakrzewska A, Boorsma A, Delneri D, Brul S, Oliver SG, Klis FM. 2007. Cellular processes and pathways that protect *Saccharomyces cerevisiae* cells against the plasma membrane-perturbing compound chitosan. *Eukaryotic Cell* **6**:600–608. DOI: https://doi.org/10.1128/EC.00355-06, PMID: 17259547

Zapater M, Sohrmann M, Peter M, Posas F, de Nadal E. 2007. Selective requirement for SAGA in Hog1-mediated gene expression depending on the severity of the external osmostress conditions. *Molecular and Cellular Biology* **27**:3900–3910. DOI: https://doi.org/10.1128/MCB.00089-07

Zhang X, Moye-Rowley WS. 2001. *Saccharomyces cerevisiae* multidrug resistance gene expression inversely correlates with the status of the F(0) component of the mitochondrial ATPase. *The Journal of Biological Chemistry* **276**:47844–47852. DOI: https://doi.org/10.1074/jbc.M106285200, PMID: 11602584

Zhang Y, Lamm R, Pillonel C, Lam S, Xu JR. 2002. Osmoregulation and fungicide resistance: the *Neurospora crassa os-2* gene encodes a *HOG1* mitogen-activated protein kinase homologue . *Applied and Environmental Microbiology* **68**:532–538. DOI: https://doi.org/10.1128/AEM.68.2.532-538.2002

Zhu J, Gong R, Zhu Q, He Q, Xu N, Xu Y, Cai M, Zhou X, Zhang Y, Zhou M. 2018. Genome-wide determination of gene essentiality by transposon insertion sequencing in yeast *Pichia pastoris*. *Scientific Reports* **8**:10223. DOI: https://doi.org/10.1038/s41598-018-28217-z

Zhu J, Zhang L, Ma D, Gao Y, Mu W, Liu F. 2019. A bioactivity and biochemical analysis of iminoctadine tris (albesilate) as a fungicide against *Corynespora cassiicola*. *Pesticide Biochemistry and Physiology* **158**:121–127. DOI: https://doi.org/10.1016/j.pestbp.2019.04.016, PMID: 31378347